Copyright © 2010 American Scientific Publishers
All rights reserved
Printed in the United States of America

Journal of
Nanoscience and Nanotechnology
Vol. 10, 1430–1449, 2010

Nanowire Photodetectors*

Cesare Soci, Arthur Zhang, Xin-Yu Bao[†], Hongkwon Kim, Yuhwa Lo*, and Deli Wang*

Department of Electrical and Computer Engineering, Jacobs School of Engineering, University of California, San Diego, 9500 Gilman Drive, La Jolla, California 92093-0407, USA

The use of nanowires and nanowire structures as photodetectors is an emerging research topic. Despite the large amount of reports on nanowire photoresponse that appeared in the literature over the last decade, the mechanism leading to high photosensitivity and photoconductive gain in high aspect ratio nanostructures has been elucidated only recently. Novel device architectures integrated in single nanowire devices are also being actively studied and developed. In this article, the general nanowire photodetector concepts are reviewed, together with a detailed description of the physical phenomena occurring in nanowire photoconductors and phototransistors, with some examples from recent experimental results obtained in our groups. An outlook on future directions toward the use of semiconductor nanowire photoconductors as intrachip interconnects, single-photon detectors, and image sensors, is also given.

Delivered by Ingenta to:
Nanyang Technological University
IP : 155.69.4.4
Mon, 10 May 2010 07:45:18

Keywords: Nanowire, Photodetector, Gain.

CONTENTS

1. Introduction 1430
2. Nanowire Photoconductors 1432
   2.1. Basic Photoconductivity Concepts 1432
   2.2. Light Absorption 1433
   2.3. Steady-State Photoconductivity 1434
   2.4. Photoconductive Gain 1435
   2.5. Nanowire Photoconductor Materials 1436
3. Nanowire Photodetectors 1440
   3.1. Photodiodes 1440
   3.2. Phototransistors 1442
   3.3. Superconductor Nanowire Photodetectors 1443
   3.4. Metal and Metal-Dielectric Nanowire Photodetectors 1444
4. Nanowire Potodetector Applications 1444
   4.1. Optical Intrachip Interconnects 1444
   4.2. Single-Photon Detectors 1444
   4.3. Image Sensors 1445
5. Summary and Conclusions 1446
   Acknowledgments 1447
   References and Notes 1447

1. INTRODUCTION

In the last decade, one-dimensional or quasi-one-dimensional nanostructures (nanowires) have been widely researched as potential building blocks for nanoelectronic circuits.[1–3] Thanks to the ongoing advancement in the growth and fabrication methodologies, by means of either top-down or bottom-up approaches, nanowires (NWs) can be now realized out of a variety of functional materials (e.g., semiconductors, metals, superconductors) and in controlled manners. On the pathway to nanoscale integration, this opens up new opportunities toward understanding and utilizing the unique physical properties of these low-dimensional systems, such as their thermoelectric properties, quantum size effects, or enhanced biological and chemical sensitivity arising from the large surface to volume ratio. One of the most studied phenomena in NWs is their sensitivity to light (photoconductivity), which is emerging as a very promising NW application for photodetectors, photovoltaics, optical switches, optical interconnects, transceivers, and biological and chemical sensing. The scope of this paper is to review recent advances in the study of the photoconductive properties of NWs and NW structures, and to give a perspective on their potential as optoelectronic components, specifically as photodetectors. Even above the quantum confinement size-regime, NW photoconductors can yield higher light sensitivity than their bulk counterparts due to the large surface-to-volume ratio and small dimensions. Moreover, the possibility to integrate functionality in NW structures, such as homo- an hetero-junctions, within single NW devices or NW arrays, enables large scale integration (for optical interconnects, transceivers etc.). Thanks to the increasingly large amount of work that has been carried on in the field (hundreds of papers were published on this topic in the last decade), we believe that a deeper understanding of the NW photoconductive properties is now being achieved, and a review of

*Authors to whom correspondence should be addressed.
[†]Present address: Department of Electrical Engineering, Center for Integrated Systems, Stanford Univeristy, Stanford, CA 94305-4075, USA.
*This is an invited review paper.

1533-4880/2010/10/1430/020 doi:10.1166/jnn.2010.2157

Cesare Soci received his Laurea (M.S. equivalent) and his Ph.D. in Physics from the University of Pavia in 2001 and 2005, respectively. He was a postdoctoral researcher at the Center for Polymers and Organic Solids at the University of California–Santa Barbara in 2005–2006. In 2006 he joined the Electrical and Computer Engineering department at the University of California–San Diego where he is continuing his postdoctoral research. He is currently an assistant professor in physics and engineering at the Nanyang Technological University in Singapore.

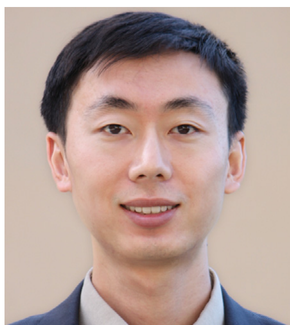

Arthur Zhang obtained his B.S. in Electrical and Computer Engineering from Cornell University in 2005. He is currently a graduate student at the University of California, San Diego, working on silicon nanowire photodetectors. He is an NSF Graduate Fellow, Jacobs Fellow at the Jacobs School of Engineering (UCSD), and a student member of IEEE EDS and LEOS.

Delivered by Ingenta to:
Nanyang Technological University
IP : 155.69.4.4
Mon, 10 May 2010 07:45:18

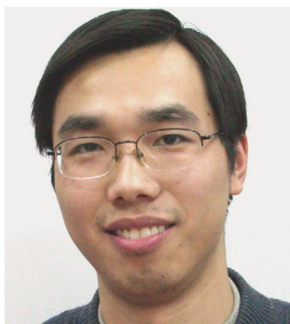

Xin-Yu Bao received his B.S. in Physics from the University of Science and Technology of China in 2001, and the Ph.D. in Physics from the Institute of Physics, Chinese Academy of Sciences in 2006. He was a postdoctoral researcher at University of California San Diego, working on III–V nanowire growth and characterization from 2006 to 2008. He is currently a postdoctoral researcher in the Department of Electrical Engineering at Stanford University working on high efficiency solar cells.

Hongkwon Kim received the B.S and M.S. degrees in electronics engineering from Pusan National University, Korea, in 1994 and 1996, respectively. He is currently pursuing the Ph.D. degree on nanowire detectors in the Department of Electrical Engineering and Computer Science, University of California, San Diego. From 1996 to 2006, he worked as a senior engineer at Samsung SDI Company Ltd., where he did research on driving method of flat panel display and integrating circuits with poly silicon thin film transistors.

Yuhwa Lo received his Ph.D. in 1987 from UC, Berkeley in Electrical Engineering and Computer Sciences. He worked at Bellcore as a member of technical staff from 1988–1990 before becoming an assistant and then associate professor of the School of Electrical Engineering, Cornell University. He became a professor of UC, San Diego since 1999 and the director of Nano3 facility of the California Institute of Telecommunications and Information Technology (Calit2) since 2006. His research interests include nanophotonics, single-photon detectors, lab-on-a-chip, biophotonics, and biomedicine. He has about 400 publications and been awarded 22 patents. He is a fellow of the IEEE and the Optical Society of America.

Deli Wang received his B.S. degree in 1990 from the University of Science and Technology of China in Material Sciences and Engineering. From 1990 to 1996, he worked in Changchun Institute of Applied Chemistry, Chinese Academy of Sciences. He earned his Ph.D. in 2001 in the Materials Department of the University of California at Santa Barbara. He then worked as a postdoctoral fellow at Harvard University. He joined the University of California–San Diego in 2004 and currently is an associate professor at the Electrical and Computer Engineering department. His research interests include rational synthesis of semiconductor nanowires and the application in electronics, optoelectronics, renewable energy, and biosensing and medicines.

NW photosensors based on material, optical, and charge transport properties will be beneficial to push fundamental research toward practical applications. We hope that a systematic comparison between state-of-the-art conventional photodetectors with NW photodetector structures could facilitate implementing new designs that gain full benefits from the unique photoconductive properties of NWs, also in view of their possible integration with CMOS technology.

Delivered by Ingenta to:
Nanyang Technological University
IP : 155.69.4.4
Mon, 10 May 2010 07:45:18

The paper is organized as follows: in Section 2 we will discuss the basic concepts of photoconductivity and photoconductive gain in NW photoconductors, putting in evidence some of the unique optical and photoconductive properties of NWs and NW arrays. We will also review some of the reports on photosensitivity in NW photoconductors grouped by material categories; in Section 3 we will present other NW photodetector concepts demonstrated in the literature, including photodiodes, phototransistors, and detectors based on superconducting or metallic NWs; finally, in Section 4, we will give an outlook on future directions in NW photodetector research, describing some possible applications such as optical intrachip interconnects, single-photon detectors, and image sensors. We provide examples from experimental results obtained in our groups to elucidate the concepts in each section.

AMERICAN SCIENTIFIC PUBLISHERS

2. NANOWIRE PHOTOCONDUCTORS

Photoconductivity is a well-known property of semiconductors in which the electrical conductivity changes (usually increases) due to the incident radiation.[4–6] Photoconductivity involves several successive or simultaneous mechanisms, namely absorption of the incident light, carrier photogeneration, and carrier transport (including carrier trapping, detrapping and recombination). The magnitude of the conductivity change induced by irradiation depends upon the number of carriers produced per absorbed photon (carrier generation quantum yield), and the mobility of photogenerated carriers. The duration of this change depends upon many factors, such as the lifetime of the carriers and the time for the carriers to encounter a trap. Therefore, photoconductivity is also a valuable probe for the electronic properties of semiconductors relating to the charge carrier mobility and lifetime. Furthermore, photoconductive semiconductors find a wide variety of applications in photodetectors and photovoltaic devices. The observation of high photoresponsivity in semiconductor NWs and recent advances in the understanding of the photoconduction mechanism in low-dimensional systems with a high density of surface states is attracting growing interest for the potential use of NWs as photosensing elements in highly integrated optoelectronic devices, hybrid organic–inorganic solar cells, optical interconnects, transceivers, etc. The basic concepts specifically related to photoconductivity in NWs, including light absorption, charge carrier photogeneration and trapping, are presented in the following.

2.1. Basic Photoconductivity Concepts

The intrinsic conductivity $[\sigma] = [\text{A/Vcm}]$ of a semiconductor in the dark is given by:

$$\sigma = en\mu \quad (1)$$

where e the electronic charge, n is the charge carrier density (for simplicity, it is assumed only one type of carriers) and μ is the carrier mobility, $[\mu] = [\text{cm}^2/\text{Vs}]$. In the presence of an applied electric field $F = V/l$ ($[F] = [\text{V/cm}]$, V is the voltage applied across a NW with length l, see Fig. 1), the current density is given by:

$$J = \sigma F = env \quad (2)$$

where $v = \mu F$ is the carrier drift velocity ($[J] = [\text{A/cm}^2]$, $[v] = [\text{cm/s}]$). Under illumination, a change in conductivity $\Delta\sigma$ (photoconductivity) might occur either due to a change in the carrier concentration Δn (carrier photogeneration) or to a change in the carrier mobility $\Delta\mu$:

$$\Delta\sigma = \sigma_{\text{light}} - \sigma_{\text{dark}} = e(\mu\Delta n + n\Delta\mu) \quad (3)$$

In general:

$$J_{\text{PC}}(t) = [\mu(t)\Delta n(t) + n(t)\Delta\mu(t)]eF \quad (4)$$

where J_{PC} is the photocurrent. Note that both, the mobility and the carrier density terms depend on time. In many

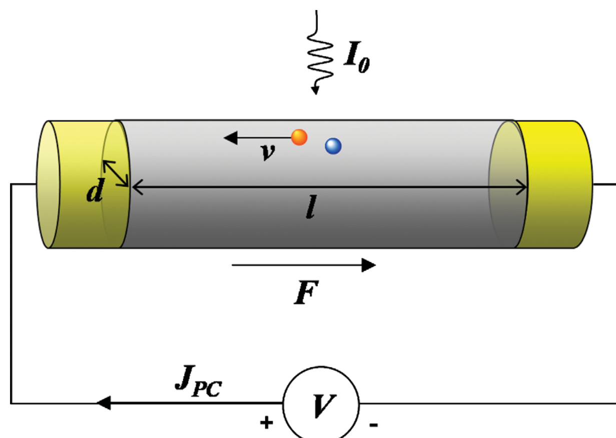

Fig. 1. Photoconductivity in NWs. I_0 is the illumination intensity, J_{PC} the current density, F the applied electric field along the current direction and v is the charge carrier drift velocity.

semiconductors $\Delta n \gg \Delta\mu$ and the time dependence of the mobility is negligible, therefore the expression for the photocurrent density reduces to the usual form:

Delivered by Ingenta to: Nanyang Technological University IP : 155.69.4.4 Mon, 10 May 2010 07:45:18

$$J_{PC}(t) = \Delta\sigma F = e\mu\Delta n(t)F \tag{5}$$

2.2. Light Absorption

Understanding the optical properties of NW materials is of large importance for the optimization of NW-based optoelectronic devices such as photodetectors and photovoltaics. While the optical properties of NWs are strictly dependent upon the dielectric functions of bulk materials, additional effects arising from the NW geometry and the low dimensionality must also be considered. These include optical birefringence, light scattering, and waveguiding effects (light funneling), which will now be discussed in more detail.

2.2.1. *Optical Birifringence and Light Polarization Effects*

In general, the absorption properties of semiconducting NWs are strongly dependent on the polarization of the incident radiation.[7,8] The direct observation of such effects on the optical function is quite challenging.[9,10] Nevertheless, these effects are easily manifested in photoconductivity and photoluminescence measurements. The two major mechanisms responsible for this phenomenon are:

(1) The modification of energy spectrum and optical matrix elements by size quantization of carriers;[11,12]

(2) The dielectric confinement of the optical electric field due to the difference in the dielectric constants of the NW ε and the environment ε_0.[7,8,13]

While the first mechanism is significant only in very thin NWs ($a < 10$ nm, where a is the NW diameter), the relevance of the latter is dictated exclusively by the ratio of $\varepsilon/\varepsilon_0$ (typically $\varepsilon/\varepsilon_0 > 10$), although it has to be treated differently whether the light wavelength exceeds the NW diameter or not. In the case of thin NWs ($a < \lambda$, i.e., $a < 100$ nm) it has been shown that the ratio of the absorption coefficient for light polarization parallel and perpendicular to the NW axis is given by:[7]

$$\frac{k_{\parallel}}{k_{\perp}} = \left|\frac{\varepsilon + \varepsilon_0}{2\varepsilon_0}\right|^2 \tag{6}$$

due to the suppression of the perpendicular component of the electric field vector inside the wire. The factor in Eq. (6) exceeds 30 for most semiconductor NWs. For thicker NWs (or at higher light frequencies), $a > \lambda$, the nonuniform distribution of the field inside the wire must also be taken into account and the ratio of $k_{\parallel}/k_{\perp}$ becomes strongly dependent upon frequency. At certain critical points, the electric field modes are purely transverse, leading to oscillations of $k_{\parallel}/k_{\perp}$ from positive to negative.[8] The case of absorption polarization anisotropy of metallic NWs and semiconductor-core/metal-shell NWs has also been discussed in Refs. [7, 8]. In these structures, because of the absorption due to plasmon resonance which is strongly polarized perpendicular to the NW axis, there is a crossover from absorption of light with parallel polarization far below the plasmon frequency to absorption of light with perpendicular polarization near and above the plasmon frequency, changing the sign of the anisotropy. In semiconductor-core/metal-shell NWs, the absorption anisotropy can be tuned from that of semiconductor NWs to that of metallic NWs by varying shell thickness and light frequency.[13]

Light polarization dependence of the photoconductivity has been experimentally observed in single NWs of a variety of material systems, including InP,[14] ZnO,[15] Si,[16] GaN,[17] *p*-Si/*n*-CdS and *p*-*i*-*n*-Si nano-avalanche photodiodes,[18,19] and InAs/InAsP axial heterojunction infrared photodetectors.[20] Anisotropy of the optical absorption results in photocurrent amplitudes varying as:

$$I_{PC} = I_{PC}^0 \cos^2\vartheta \tag{7}$$

where ϑ is the light polarization angle respect to the principal NW axis. Strong dependence of optical absorption on light polarization is therefore to be expected also in ordered NW arrays, where NWs can be either aligned horizontally or vertically with respect to the substrate. Furthermore, similar to the well understood phenomenon of polarization memory in photoluminescence from optical anisotropic media, polarization dependence of the photocurrent upon selective excitation has also been observed in CdSe and CdTe NW meshes (i.e., collection of NWs randomly distributed between two electrodes), where the applied electric field dictates a preferential charge carrier transport direction.[21,22]

2.2.2. Light Scattering and Absorption Enhancement in Vertical NW Arrays

Enhanced light scattering is expected in NW structures, when the physical dimensions become comparable to or significantly smaller than the wavelength of the incident radiation. Because of the intrinsic anisotropy of NWs, enhanced light scattering can lead to interesting phenomena such as giant optical birefringence[23] or optical funneling.[24,25] Effective-medium models predict a significant reduction of the reflectance of vertical NW arrays over the entire spectral range, due to the low effective refractive index of the array of NWs surrounded by air (the NW array acts as a stepped-index antireflection coating).[24,26] However, for closely packed NW structures, the electromagnetic interaction between NWs cannot be neglected when evaluating their optical properties. Numeric calculations have shown that Si NW arrays approach total absorption of incident light at small wavelengths,[24,25] due to the confinement of the electromagnetic energy into the high refractive index NW volume (light funneling), thus outperforming their thin film counterparts.

Figure 2 shows the results of numeric simulations of the optical absorption in 2D Si NW arrays, demonstrating that the percentage of photon energy within the NW volume can be significantly larger than the physical fill factor, especially at large pitches.[25] At longer wavelengths, however, the reduction of the Si extinction coefficient is not fully compensated by the decrease in reflectance, so that the physical fill factor of the NW array must be carefully designed in order to approach the overall absorption efficiency of its thin film counterpart.[24] Recently the optical properties of vertical arrays of InP, Si, and GaP NWs have been investigated experimentally.[26] It was found that, for typical NW diameters around 50 nm, diffuse multiple light scattering dominates the optical properties of the NW arrays, and that depending on the ratio between the absorption and scattering mean free path (the latter can be controlled by varying the NW diameter or by infiltration with refractive index matching materials), absorption losses can be strongly suppressed in the NW arrays. This has obvious implications for the design of efficient NW absorbers in NW-based photovoltaic cells, or in determining the spectral response of NW photodetectors.

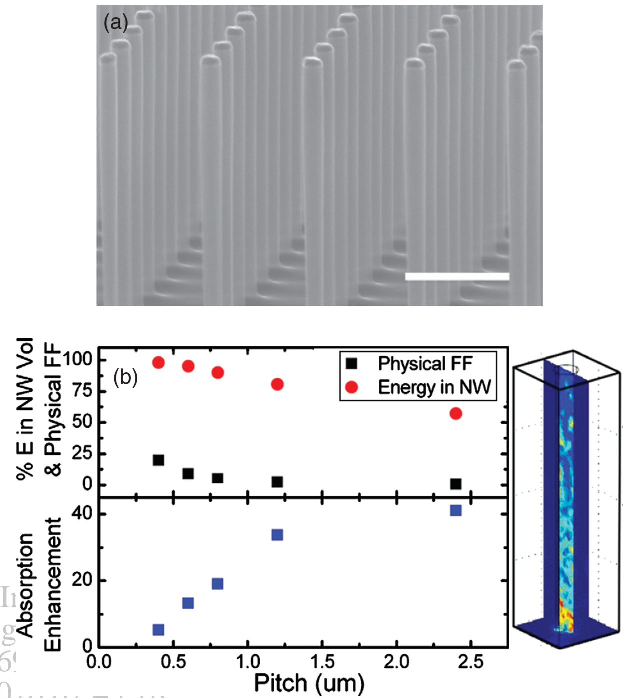

Fig. 2. (a) SEM of vertical-etched Si NW array device. The wires are 200 nm in diameter and 2.7 μm in length with 1 μm spacing. Scale bar is 1 μm. (b) Upper plot: the electric field energy inside 2D Si NW arrays with varying pitch. The presence of the higher index NW enhances the energy inside the wires above the physical fill factor. Lower plot: absorption enhancement in the NW array (ratio of the percentage of total energy absorbed in the NW to physical fill factor), as a function of pitch. As pitch increases, the light funneling effect becomes more pronounced. On the right: a visual representation of the energy confinement into the NW volume. Reprinted with permission from [25], A. Zhang et al., *Appl. Phys. Lett.* 93, 121110 **(2008)**. © 2008, American Institute of Physics.

2.3. Steady-State Photoconductivity

In the simplest scenario where direct carrier photogeneration is achieved by continuous linear optical excitation of an interband transition, light absorption is described by the Lambert-Beer's law:

$$\frac{dI}{dz} = -\alpha I, \quad I(z) = I_0 e^{-\alpha z} \tag{8}$$

where α ($[\alpha] = [\mathrm{cm}^{-1}]$) is the absorption coefficient, I_0 the illumination intensity ($[I] = [\mathrm{W/cm^2}]$) and z is the direction along which absorption occurs. A cylindrical NW, with diameter d and length l, is characterized by the geometrical parameters summarized in Table I, where $A = 2A_{\emptyset} l/d$. The average optical generation rate over the thickness of the NW would then be:

$$g_d = \eta^*(P_{\mathrm{opt}}/\hbar\omega)/\mathrm{Vol} = 2\eta^*(P_{\mathrm{opt}}/\hbar\omega)/Ad \tag{9}$$

where $P_{\mathrm{opt}} = I_0 A$ ($[P_{\mathrm{opt}}] = [W]$) is the incident optical power on the slab surface area and $\eta^* = \eta\eta^\dagger$ is the effective carrier photogeneration quantum efficiency ($\eta^\dagger$ accounts for the effects of light reflection, light scattering and low-dimensionality on the NW absorption—see Section 2.3—and η is the quantum efficiency—see below). Photoexcited carriers will eventually relax to the ground state with a characteristic lifetime τ. Therefore, at steady-state under constant illumination, the density of

Table I. Geometrical parameters of cylindrical NW photoconductors.

Exposed surface area	Cross-sectional area	Volume
$A = \frac{1}{2}2\pi r l = \pi d l/2$	$A_{\emptyset} = \pi r^2 = \pi d^2/4$	$\mathrm{Vol} = \pi r^2 l = \pi d^2 l/4 = A_{\emptyset} l = Ad/2$

photogenerated carriers ($[n] = [\text{cm}^{-3}]$) will be:

$$\Delta n(t) = g_d \tau = \text{const.} \tag{10}$$

It follows that the photoconductivity (Eq. (3)) is given by:

$$\Delta\sigma = g_d e(\mu\tau) \tag{11}$$

The mobility-lifetime product ($\mu\tau$) is often taken as a figure of merit for photoconductors, indicating their sensitivity to photoexcitation.[6] By combining Eqs. (5) and (9), the total steady-state PC density in the NW, for a given photon energy, can be written as:

$$J_{\text{PC}} = \Delta\sigma F = 2\eta^*(P_{\text{opt}}/\hbar\omega)eF\mu\tau/Ad \tag{12}$$

Equation (12) is easily generalized to the case where two types of charge carriers, e.g., electrons and holes with carrier density n and p, respectively, contribute to the photocurrent response across the area $A_\emptyset$ ($[I_{\text{PC}}] = [\text{A}]$):

Delivered by Ingenta to:
Nanyang Technological University
IP : 155.69.4.4
Mon, 10 May 2010 07:45:18

$$I_{\text{PC}} = J_{\text{PC}} A_\emptyset = \eta^*(P_{\text{opt}}/\hbar\omega)eF(\mu_n\tau_n + \mu_p\tau_p)/l \tag{13}$$

We notice that, due to the cancellation of the geometrical terms describing the cylindrical photoconductor geometry, Eq. (13) coincides with the well-known expression for photocurrent in a bulk semiconductor slab. This would not be the case, for instance, in a cylindrical transverse photoconductor where the electrodes are arranged axially (refer also to core–shell NW structures in Section 3.1). In such structures, with a central electrode of radius r_0 and a peripheral electrode separated by a distance M, the photocurrent would be increased by a factor of $8/\ln(M/r_0)$ compared to a planar photoconductor with comparable device size (i.e., $l = 2M$).[27]

2.4. Photoconductive Gain

The mechanism leading to high light sensitivity in photoconducting NWs has been recently discussed in Refs. [28–34]. Because of the large surface-to-volume ratio, NWs contain an extremely high density of surface states. Consequently, due to the pinning of the Fermi energy at the surface, NWs exhibit a depletion space charge layer which provides physical separation of electrons and holes and can lead to significantly enhanced photocarrier lifetime (persistent photoconductivity). Since the carrier distribution inside the NW is mainly determined by the surface potential and Fermi energy pinning, which strongly depend on the geometry of the wire, the dark- and photo-currents in NWs vary considerably with their size. Theoretical calculations for InP NWs have shown that small diameters (i.e., minimal band bending) result in full-depletion of the NWs, thus minimize the dark current (the predominant source of noise in photodetectors), while large diameters (i.e., appreciable band bending) increase the photoconductivity by hindering photogenerated carrier recombination.[29] Consistent results have been experimentally observed in GaN NWs with different diameters ranging from ~50 to 500 nm,[28] as well as in SnO_2 NWs.[35] A schematic of surface state effects on band bending and photogenerated carrier separation in n-type NWs with different diameters is depicted in Figure 3.

An alternative way to define the sensitivity of a photoconductor is in terms of the number of charge carriers which pass between the photoconductor electrodes per second (N_{el}, $[N_{\text{el}}] = [\text{s}^{-1}]$) for each photon absorbed per second that creates an electron–hole pair (N_{ph}, $[N_{\text{ph}}] = [\text{s}^{-1}]$). This ratio defines the photoconductive gain, G:

$$G = \frac{N_{\text{el}}}{N_{\text{ph}}} = \frac{I_{\text{PC}}/e}{P_{\text{abs}}/\hbar\omega}, \quad P_{\text{abs}} = \eta^* P_{\text{opt}} \tag{14}$$

where P_{abs} is the power absorbed in the photoconductor that results in the photogeneration of electron–hole pairs ($[P_{\text{abs}}] = [W]$). By combining Eqs. (14) and (12) one obtains:

$$G = \frac{F\mu\tau}{l} = \frac{\tau}{\tau_t} \tag{15}$$

where $\tau_t = l/v = l/\mu F = l^2/\mu V$ is the carrier transit time (Fig. 1). Semiconductor NWs show extremely high photoconductive gain due to a combination of the following:
(1) the photocarrier lifetime is considerably prolonged due to charge separation promoted by surface states;
(2) the carrier transit time is significantly reduced due to the high mobility achievable in high-quality, defect-free single crystal NWs combined with small interelectrode distances.[30, 31]

Physically, the process leading to photoconductive gain can be envisioned as follows: free electron–hole pairs are generated after photoexcitation. If the lifetime of a carrier is greater than its transit time, it will make several effective transits through the material between the contacts, provided that the contacts are ohmic and are able to replenish carriers drawn off at the opposite contact by the injection of an equivalent carrier. In effect, the free carrier continues

AMERICAN SCIENTIFIC PUBLISHERS

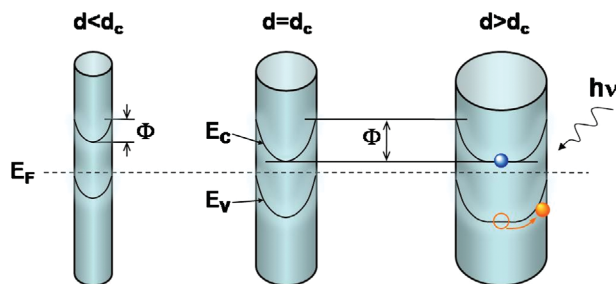

Fig. 3. Schematic of the dependence of valence (E_V) and conduction (E_C) band profiles in NWs with different diameters d. Below the critical diameter d_c, the NW is fully depleted and band bending is minimal. For larger diameters, the recombination barrier Φ increases, thus the photocarrier lifetime is prolonged. The detail on the right shows the charge carrier separation mechanism upon photoexcitation. Adapted with permission from [28], R. Calarco et al., *Nano Lett.* 5, 981 (**2005**). © 2005, American Chemical Society.

to circulate until it is annihilated by either recombination or trapping.

If both, electrons and holes contribute to the conductivity, then:

$$G = \frac{F(\mu_n\tau_n + \mu_p\tau_p)}{l} = \frac{V(\mu_n\tau_n + \mu_p\tau_p)}{l^2} \tag{16}$$

By using Eq. (16), the photocurrent (Eq. (13)) can also be written as:

$$I_{\text{PC}} = e\frac{P_{\text{abs}}}{\hbar\omega}\frac{\tau}{\tau_t} = e\frac{P_{\text{abs}}}{\hbar\omega}G \tag{17}$$

A photoconductor with internal gain can be considered as an equivalent current amplifier, in which the bandwidth for a response time τ is $B = 1/2\pi\tau$. The gain-bandwidth product of the photoconductor, therefore, is given by:

$$GB = \frac{\tau}{\tau_t}\frac{1}{2\pi\tau} = \frac{1}{2\pi\tau_t} \tag{18}$$

Delivered by Ingenta to: Nanyang Technological University IP : 155.69 Mon, 10 May 20

The achievement of photoconductive gain greater than unity requires the presence of ohmic contacts. From Eq. (16) it is evident that one way to increase the gain is to increase the applied voltage in order to decrease the carrier transit time. However, the maximum achievable value for the carrier transit time, hence for the gain, in the absence of traps would be limited by the dielectric relaxation time, τ_d, of the photoconductor;[4–6] higher values for the gain and the gain-bandwidth product can be obtained in the presence of deep traps (i.e., below the Fermi level) or recombination centers, as those that are usually created by surface states in NW photoconductors. For example, in the case of minority carriers being deeply trapped and majority carriers being free to move and to be injected into the photoconductors from the ohmic contacts, it is possible to obtain $\tau_t > \tau_d$.

In our previous study on the photoconductivity of ZnO NWs, we have found that substantial photoconductive gain, as high as $G \sim 10^8$, could indeed be achieved in these nanostructures (Fig. 4(a)). Despite the slow relaxation time ($\tau \sim 10$ s), the extremely high photoconductive gain resulted in gain-bandwidth products of $GB > 10$ GHz, as confirmed by the fast photocurrent response measured in the sub-nanosecond time domain (Fig. 4(b)).[31] Recent analyses of photoconductivity in ZnO NWs have confirmed our results.[33,34] Moreover, ultrahigh photocurrent gain ($G \sim 10^5$) has also been observed in m-axial GaN NWs,[32] although its origin was identified in the strong surface electric field present in GaN NWs that facilitates photogenerated charge separation, rather than on the effect localizing surface trap states.[28,32] All these studies indicate that the one-dimensional or quasi-one-dimensional geometry of NW photoconductors can consistently yield photoconductive gain at least three orders of magnitude larger than their thin film counterparts, as a result of the long photocarrier lifetimes.[32,33] Large photoconductive gain is achieved at the expense of dynamic response, although optimization of the electrode geometry to minimize carrier transit time can allow achieving simultaneously high sensitivity and large gain-bandwidth products. For comparison, typical response times and gain values of conventional and NW photodetectors are summarized in Table II.[36,37]

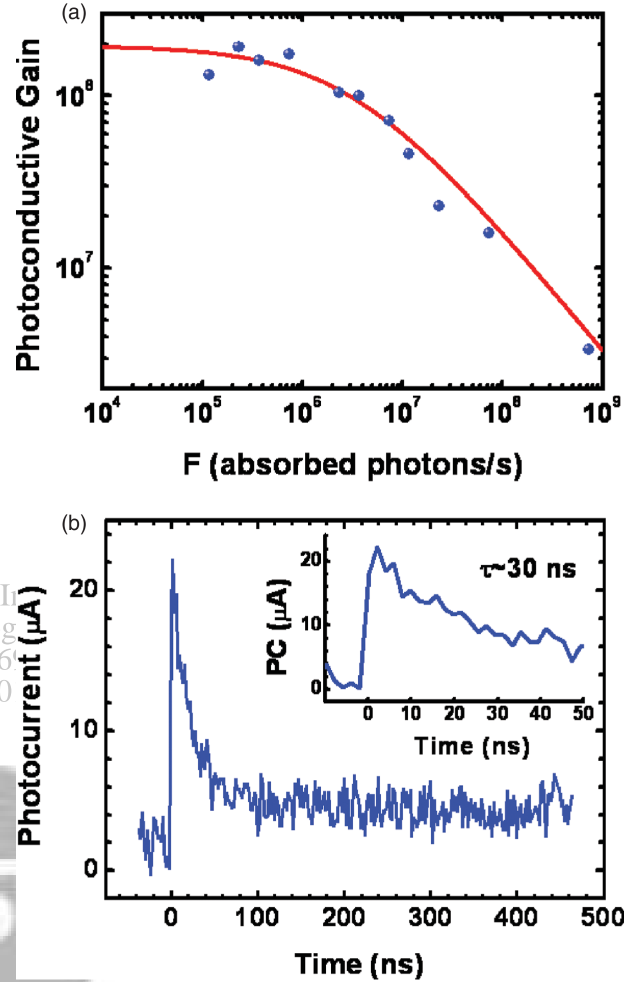

Fig. 4. (a) Photoconductive gain relative to the photon absorption rate extracted from photocurrent measurements in a single ZnO NW device with 5 V applied bias. (b) Fast transient photocurrent (PC) waveforms of ZnO NWs. The excitation intensity was $I = 0.3$ μJ/pulse and the applied bias 1 V. The inset of (b) shows the initial photocurrent decay in air, from which a characteristic time of ~30 ns can be inferred. Reprinted with permission from [31], C. Soci et al., *Nano Lett.* 7, 1003 **(2007)**. © 2007, American Chemical Society.

2.5. Nanowire Photoconductor Materials

NW photoconductors are the simplest configuration of NW-based photodetectors. Generally, single NWs or NW mashes (either randomly distributed, or aligned along a preferential direction) are dispersed horizontally on an insulating substrate, and external bias is applied between top metal electrodes. Upon illumination (with light impinging perpendicular to the NW axis) the electrical conductivity increases, thus providing light-sensing capabilities.

Table II. Typical values of response time and internal gain of photodetectors.

Detector	Response time [s]	Gain
Photoemissive		
Diodes	10^{-11}	1
Photomultipliers	$10^{-10}-10^{-8}$	10^{6}
Photovoltaic		
p-n junction	10^{-11}	1
p-i-n junction	$10^{-10}-10^{-8}$	1
Schottky junction	10^{-11}	1
Phototransistors	$10^{-8}-10^{-7}$	10^{2}
Avalanche photodiodes	$10^{-10}-10^{-6}$	$10^{2}-10^{6}$
Photoconductor		
Bulk	$10^{-8}-10^{-3}$	$1-10^{6}$
Nanowires	$10^{-11}-10^{2}$	$1-10^{10}$

Source: Adapted with permission from [36], F. Stockmann, *Appl. Phys.* 7, 1 (**1975**). © 1975, Springer-Verlag; from [37], S. M. Sze, Physics of Semiconductor Devices, Wiley, New York (**1981**). © 1981, Wiley.

The unique properties of individual NWs or vertical arrays of NW photoconductors, such as light polarization sensitivity, light absorption enhancement, and internal photoconductive gain, could be exploited for the realization of efficient and highly integrated devices such as optical switches, optical interconnects, or image sensors. Both the device geometry (as discussed in the previous section) and the intrinsic material properties (such as charge carrier density and mobility) play a fundamental role in determining the overall photoresponse of NW photoconductors. Here we will focus on the latter by briefly reviewing the properties of NW photoconductors based on material categories.

2.5.1. Group III–V Compounds

III–V compound semiconductors are among the most promising materials for NW photodetectors, due to their excellent transport properties, ease of doping, and the possibility to tune their optical absorption over a wide spectral range by alloy bandgap engineering. Nevertheless, reports on the photoconductive response of III-arsenide NWs are somehow lacking,[38–40] most likely due to the difficulty in obtaining intrinsic NW crystals (with low dark current) and to the strong effect of surface states which often causes full depletion of the NWs. One of the earliest reports of photodetection from a single InP NW appeared in year 2001, together with the observation of significant polarization anisotropy (see discussion in Section 3.2).[14] Studies on the photoconductivity of III-hydrides compound NWs have been focused primarily on their ultrafast photocarrier dynamics.[39–41] GaAs, AlGaAs and InGaAs NWs were studied by time-resolved terahertz spectroscopy, showing ultrafast charge carrier relaxation in the picosecond time domain.[39,40] More recently, fast (14 ps FWHM at 780 nm) photoconductive response has been demonstrated in an intersecting array of InP NW grown in a coplanar waveguide transmission line.[41] These studies have highlighted the potential of III–V compound semiconductor NWs for the fabrication of high-speed photodetectors.

III-nitride based NWs have also been attracting increasingly more attention for ultraviolet photodetection, which could potentially be extended to the entire visible spectral region by alloying with InN. Similar to metal-oxide NWs, networked GaN NWs have shown strong sensitivity to the ambient conditions (air vs. vacuum)[42] and the existence of persistent photocurrents,[17,42] which advert to the importance of surface states (possibly originating from nitrogen vacancies) in forming deep-level traps. As pointed out earlier, surface states play a major role in determining the photocarrier lifetime, and ultimately the NW photoconductive response. As a result, the photocurrent density may strongly depend on NW diameter, as was observed in GaN NWs where, due to the presence of a surface depletion space charge layer, carrier lifetime is greatly prolonged in NWs with diameter larger than 100 nm (leading to persistent photoconductivity) while is significantly reduced in smaller diameter NWs due to enhanced surface recombination.[28]

Delivered by Ingenta to: Nanyang Technological University IP : 155.69.4.4 Mon, 10 May 2010 07:45:18

2.5.2. Group IV

The Group IV semiconductors most commonly used in devices comprise of Si and Ge. Si has been the material of choice for visible light detection for many years due to its well known material properties and ease of fabrication in line with CMOS processing. Si NW based photoconductive devices have been fabricated through both chemical synthesis[16,43,44] and etch-back methods,[25,45,46] followed by standard lithographic processes. In most of the cases, these devices have shown large photoconductive gain which saturates at high irradiation intensities.[45] Typical rise and decay times in intrinsic NWs are less than 100 μs, but they greatly increase with doping due to the formation of midgap states created by defects in the crystalline structure.[44] The photoresponse depends significantly on the device geometry and contacts; Schottky-like contacts to the NWs can lead to a spatial dependence of the photoresponse, with higher sensitivity near the contacts (see also Section 2.1).[16] Ge is widely used in bulk and thin film photodetectors, and is extremely valuable in detection of optical communication wavelength of 1550 nm. Surprisingly, sparse literature showed photoresponse from a dense array[47] or from individual[48] Ge NWs upon visible illumination only. From the available data, Ge NWs displayed photocurrent rise and decay kinetics with time constants much longer than bulk Ge, with multiple components ranging from sub-milliseconds to seconds.[47,48]

2.5.3. Group VI

Hystorically, Se has been one of the most studied photoconducting materials. After the discovery of photoconductivity in amorphous Se by Smith in 1873,[49] Se has found

important commercial applications in xerography. One of the main advantages of Group VI semiconductor NWs, including Se and Te, is the availability of solution-based synthetic methods,[50,51] which could potentially allow low-cost and large scale production of NWs on a variety of host substrates. Large photoconductive increase (up to ∼150 times) has been shown in trigonal Se NWs upon exposure to tungsten light, and the photoconductive response was found to saturate at high light intensities.[50] Photoactive Te NWs have also been studied in a multilayer Te NW/polyelectrolyte thin solid film. Extremely long rise and decay times of the photoconductance of about 40 s were also observed in this case, although retardation of charge transfer in the complementary polyelectrolyte layers was suspected to play a role.[51]

2.5.4. Group II–VI

II–VI semiconducting compounds (sulfides, selenides, and tellurides) are widely employed in optoelectronic applications due to their direct bandgap and a wide coverage of bandgap energies. $Hg_{1-x}Cd_xTe$, for instance, is one of the most important semiconductor materials for infrared detection since its bandgap can vary monotonically over a wide spectral range, from the far-infrared to 1.5 eV. Wide bandgap II–VI materials, such as CdTe, ZnTe, CdSe, ZnSe, and CdS are typically used for visible light detection instead. A large variety of II–VI semiconductor NWs has been synthesized by different methods, and showed significant photoresponse in the infrared, visible, and ultraviolet spectral range. "Normally-on" infrared photodetectors have been realized by using electrochemically self-assembled CdS and ZnSe NWs electrodeposited in porous alumina. In these devices, the NW resistance abnormally increased up to two orders of magnitude upon exposure to infrared radiation (negative photoreponse), most likely due to photoinduced electron trapping from the semiconductor NWs to the surrounding alumina.[52] CdS NWs and nanobelts are among the most studied photoconductors in group II–VI for visible and ultraviolet light detection.[53] Similar to the case of metal-oxide NWs, the photoresponse of CdS low-dimensional structures is strongly affected by surface oxygen photochemistry, which can significantly alter the photocarrier relaxation dynamics.[30,54–56] The quantitative measurement of the electron and hole mobility-lifetime products of CdS NWs using scanning photocurrent microscopy has also provided experimental evidence that carrier lifetime is increased in NWs compared to the bulk material.[57,58] The photoconductive properties of CdSe NWs have also been reported. The large spontaneous polarization of CdSe, combined with the highly anisotropic shape of NWs, results in permanent dipole moments that have been exploited for dielectrophoretic alignment of these structures into NW photodetectors.[59] Metal-CdSe-metal NW structures have also been assembled by a template growth method, which showed significant photosensitivity upon white light illumination.[60] Long rise and decay times of the photocurrent (of ∼1 s and ∼200 μs, respectively) were also observed in this case. As already mentioned in Section 2.2, strong light polarization sensitivity in group II–VI NWs has been observed not only in ordered ensembles of CdSe NWs,[59] but also in random networks of CdSe and CdTe NWs.[21,22] Both single ZnSe NWs[61] and arrays of free-standing ZnSe NWs[62] were studied as visible light detectors. An extremely high responsivity, greater than 20 A/W at 400 nm excitation wavelength, was obtained from the single NW device. In both cases, the photocurrent showed persistent behavior with slow relaxation components attributed to the presence of deep traps.[61,62]

2.5.5. Metal Oxides

Metal-oxide NWs are an extremely important class of photoconductors. Due to their wide bandgap, metal-oxide NWs are attracting a lot of attention for the realization of transparent conducting electrodes and UV photodetectors. Furthermore, the strong influence of surface chemistry on the conductive and photoconductive properties of metal-oxide NWs makes them especially suitable for gas and chemical sensing.

A combination of ease of synthesis and attractive optical, mechanical, and magnetic properties makes ZnO one of the most interesting NW materials; photoconductivity is arguably the most studied of ZnO NW properties. Due to the wide bandgap ($E_g = 3.34$ eV at room temperature), ZnO NWs may find application in visible-blind UV photodetectors. Additionally, the presence of oxygen vacancies sometimes results in deep level donor states manifested in a "green" photoluminescence and photoconductivity band, which may be exploited to extend the spectral sensitivity of ZnO to the visible range.[15,63–65] Both, single NW or NW bundles, and vertical NW array ZnO photodetectors have been extensively investigated. In one of the earliest reports on single ZnO NW photodetectors, high photoconductive response (4 to 6 orders of magnitude decrease in resistivity) has been observed upon exposure to UV light (365 nm),[66] with extremely long photocurrent relaxation times (of the order of seconds), related to carrier trapping. Indeed, the material quality (i.e., the density of defect states) was found to have a significant impact on photocarrier lifetime and photoresponse speed.[67] It is known that photoconduction in ZnO NWs is governed by a charge-trapping mechanism mediated by oxygen adsorption and desorption at the surface (Fig. 5(a)):[15,31,68–76] in the dark, oxygen molecules are adsorbed on the oxide surface and capture the free electrons present in the n-type oxide semiconductor, and a low-conductivity depletion layer is formed near the surface:

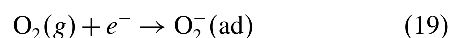

$$O_2(g) + e^- \rightarrow O_2^-(\text{ad}) \tag{19}$$

Delivered by Ingenta to: Nanyang Technological University IP: 155.69.4.4 Mon, 10 May 2010 07:45:18

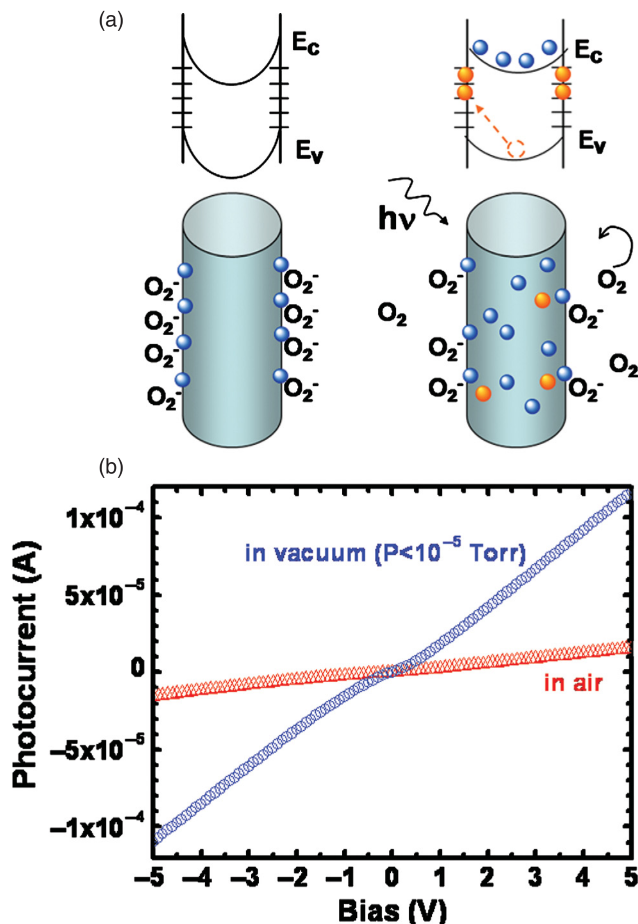

Fig. 5. (a) Trapping and photoconduction mechanism in ZnO NWs. Oxygen molecules adsorbed at the NW surface capture the free electron present in the *n*-type semiconductor forming a low-conductivity depletion layer near the surface and, under UV illumination, photogenerated holes migrate to the surface and are trapped, leaving behind unpaired electrons in the NW that contribute to the photocurrent. The lifetime of the unpaired electrons is further increased by oxygen molecules desorption from the surface when holes neutralize the oxygen ions. The top drawings show a schematic of the energy band diagrams of the NW in the dark and under illumination, indicating band-bending and surface trap states. E_V and E_C are the valence and conduction band, respectively. (b) I–V characteristics of a single ZnO NW under UV illumination measured in air (triangles) and in vacuum, at $P < 10^{-5}$ Torr (circles). Reprinted with permission from [31], C. Soci et al., *Nano Lett.* 7, 1003 **(2007)**. © 2007, American Chemical Society.

Upon illumination at photon energies above E_g, electron–hole pairs are photogenerated [$h\nu \rightarrow e^- + h^+$]; holes migrate to the surface along the potential slope produced by band bending and discharge the negatively charged adsorbed oxygen ions, and consequently oxygen is photo-desorbed from the surface:

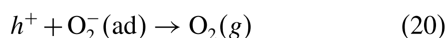

$$h^+ + O_2^-(\text{ad}) \rightarrow O_2(g) \quad (20)$$

The unpaired electrons are either collected at the cathode or recombine with holes generated when oxygen molecules are re-adsorbed and ionized at the surface. By prolonging the photocarrier lifetime, this mechanism further enhances the NW photoresponse and leads to extremely high photoconductive gain (Section 2.4). This also causes saturation of the photoresponse at high illumination intensity due to the reduction of the number of available hole-traps and consequently to the shortening of the carrier lifetime.[31] The pronounced effect of surface oxygen photochemistry on the photoconductivity of ZnO NWs has potential application in gas sensing. Typically, the photoconductance decreases with increasing oxygen pressure (due to the increased depletion of electrons in the NW) and increases with increasing temperature (due to increased oxygen desorption).[31, 68, 69, 73, 74, 77, 78] The strong influence of the environmental conditions (ambient air and vacuum) on the photoconductivity of one of our ZnO NW devices is illustrated in Figure 5(b).

Vertical ZnO NW arrays allow larger surface coverage and high NW density, thus larger photocurrent signals. NWs are typically grown from a ZnO buffer layer (which serves as a first electrode) deposited on a substrate (such as glass, sapphire or Si) by chemical vapor deposition[78–81] or solvothermal[77] methods. NWs can then be covered by a top ZnO layer[78] or infiltrated with a filling material (such as spin-on-glass)[80] to allow deposition of the top electrode without shortage. Alternative fabrication procedures such as flip-chip,[79] microfluidic pattering,[82] or NW growth in the channels of anodized alumina membranes,[83] have also been explored. The latter in particular has allowed studying the effects of the interaction of ZnO NWs with the surrounding alumina layer: negative photoconductance was observed in pristine samples due to photogenerated electron tunneling to the alumina (which is known to provide electron trapping states), which could be reverted to positive photoconductance by reducing the alumina impurity level by thermal annealing in Ar gas.

Besides ZnO, a variety of other metal-oxide NW photoconductors have also been investigated, among which are gallium, tin, indium, cadmium, and vanadium oxides. Ultra-wide bandgap gallium oxide NWs, such as β-Ga_2O_3 ($E_g = 4.2$–4.9 eV),[84] or zinc-gallate, $ZnGa_2O_4$, NWs ($E_g = 4.4$–4.7 eV),[85] are of great technological interest for the development of visible-blind photodetectors. These materials were recently synthesised in the form of NWs and their UV photoresponse has been charachterized.[84, 85] NW photodetector responded selectively to UV radiation and, in the case of zinc-gallate NWs, the photoresponse was strongly dependent on oxygen chemisorption. SnO_2 NWs ($E_g = 3.6$ eV) are also used as UV photodetectors.[35, 86, 87] Similar to the other metal-oxides, the surface photochemistry affects the intrinsic conductance of SnO_2 NWs, and results in extremely long (up to 300 s) photocarrier lifetimes, which strongly depend on NW diameter[35] and ambient conditions.[76, 87] In_2O_3 NWs (direct bandgap: $E_g^d = 3.75$ eV and indirect bandgap: $E_g^i = 2.62$ eV) have also shown similar photocurrent dynamics and dependence on O_2 environment, and up to four orders of magnitude

increase in conductance upon exposure to UV light. Interestingly, a phonon-assisted sub-gap photocurrent was also detected with illumination at photon energy of ~3.4 eV in this case.[88] Photoresponse via excitation of the indirect bandgap was also observed in CdO NWs ($E_g^d = 2.27$ eV, $E_g^i = 0.55$ eV), which was used for detection of infrared radiation; in this case the photoconductance was suppressed by exposing the NW detector to NO_2 gas diluted in Ar.[89] V_2O_5 NWs showed a weakly temperature-dependent persistent photocurrent upon exposure to white light, that was interpreted in terms of hopping-mediated transport.[90]

3. NANOWIRE PHOTODETECTORS

Apart from NW photoconductors, in which the photoconductive gain mechanism is inherently present due to the large surface to volume ratio, other one-dimensional or quasi-one-dimensional photodetector structures based on semiconducting, superconducting or metallic NWs, are being actively investigated for efficient conversion of optical to electrical signals. Conventional photodetector concepts and architectures (e.g., semiconductor *p-n* or *p-i-n* photodiodes) are being replicated in NW structures, where homo- and hetero-junctions are either formed directly during the NW growth (bottom-up approach), or prior to the NW fabrication (top-down approach), to create highly sensitive photodetectors with potential for denser integration, higher specificity, and responsive to light polarization. Additionally, novel concepts arising from the large surface to volume ratio (e.g., in NW phototransistors) or from the small NW dimensionality (e.g., in metal and superconductor photodetectors) are proposed to enhance photosensitivity, and ultimately reach single-photon detectivity. Some of the principal NW photodetector concepts demonstrated in the literature are reviewed in the following.

3.1. Photodiodes

NWs offer a variety of opportunities to form photodiode architectures, including Schottky metal-semiconductor junctions and homo- or hetero-junction devices formed either axially along the NW (Fig. 6(a)), or radially by conformal NW coating (core–shell junctions, Fig. 6(b)). Moreover, the possibility to create "crossed" (Fig. 6(c)) and "branched" NW junctions,[91] or to directly grow vertical NW arrays on a variety of substrates (Fig. 6(d)) largely enriches the sample of device architectures and material combinations available for the realization of NW photodetectors.[92] It is worth noticing that, depending whether illumination is perpendicular (Figs. 6(a, d)) or parallel (Figs. 6(b, c)) to the junction plane, the boundary conditions for the continuity equation describing carrier diffusion across the junction at steady-state will vary

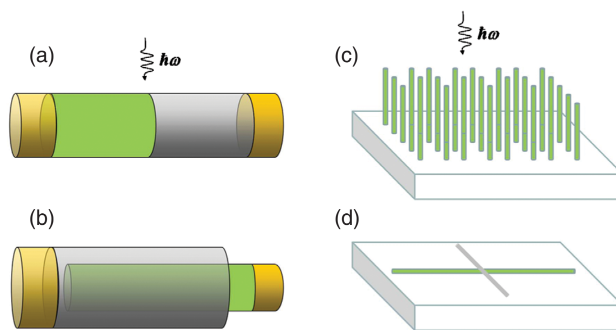

Fig. 6. (a) Axial NW junction; (b) Core/shell, radial NW junction; (c) Vertical NW array heterojunctions formed with the growth substrate; (d) "Crossed" NW junction. The segments in different colors represent either different doping or different materials for homogeneous and heterogeneous junctions, respectively.

considerably.[93] Furthermore, in the case of light impingement parallel to the junction plane the effects of non-uniform absorption across the junction should also be considered.

Delivered by Ingenta to: Nanyang Technological University IP: 155.69.4.4 Mon, 10 May 2010 07:45:18

Recently, a lot of interest has arisen for NW photodiodes operated in photovoltaic mode for solar power conversion.[94,95] These include single Si NW homojunctions[96] (either axial[97,98] or radial[99]), vertical NW array homo- and hetero-junctions (such as *n*-Si NWs/*p*-Si substrate,[100] *p*-Si NWs/*n*-amorphous-Si,[101] or *p*-GaN NWs/*n*-Si substrate[102]), and vertical NW arrays of core/shell homo- and hetero-junctions (such as *n*-core/*p*-shell GaAs NWs on *n*-GaAs substrate[103] or ZnO-core/ZnSe-shell NWs on transparent conductive oxide substrate[104]). For the sake of brevity, studies specifically aimed at photovoltaic applications will not be discussed here, whereas the reader is referred to the literature referenced above. Nevertheless, we will review in more details the major NW photodiode structures used for photodetector applications, including *p-n* and *p-i-n* photodiodes, Schottky diodes, and other heterojunction devices.

AMERICAN SCIENTIFIC PUBLISHERS

3.1.1. Homogeneous and Heterogeneous Junctions

Both homo- and hetero-junction single NW photodiodes (Fig. 6(a)) have been demonstrated. For instance, UV photodetectors based on single GaN NWs including axial *p-n* homojunctions have shown rectifying behavior, relatively fast photoresponse, and a photoconductive increase of about 14 under 0.03 V reverse bias.[105] Similarly, IR photodetectors based on single NWs including InAs/InAsP axial heterojunctions operated at 77 K exhibited very low dark current (due to the conduction band offset formed at the NW heterointerface), strong polarization dependence, and a combined contribution to the photoconductive response from the InAs portion (with onset around 0.5 eV) and from the InAsP portion (with tunable onset from 0.65 to 0.82 eV depending on the phosphorous content).[20]

As previously mentioned, core–shell NW junctions (Fig. 6(b)) are attracting a lot of interest for photovoltaic

applications, although similar design concepts could be implemented for more efficient photosensing schemes that take advantage of the more effective charge carrier separation, and possibly of the enhanced light absorption in vertical arrays expected from radial NW junctions.[94] So far, efficient photoresponse has been demonstrated in both a single Si NW[99] and a vertical GaAs NW array[103] with radial homojunctions. Type-II core/shell NW heterostructures have also been proposed[95] and demonstrated[104] to promote charge carrier separation, improve the photosensitivity and additionally enhance the spectral response.

Photodetectors based on heterogeneous junctions formed by vertical NW arrays with their growth substrates (Fig. 6(c)) have also been investigated, where large NW densities are desirable to increase the photoactive area and thus enhance the photoconductive response. In particular, due to the ease of fabrication by a variety of methods, including chemical vapor deposition,[106, 107] solvothermal methods,[108] or magnetron sputtering,[109] a substantial amount of work has been dedicated to heterojunction photodetectors made of ZnO NWs on doped Si substrates. In these structures, depending on the density of the NW network, the top electrode can be either deposited directly onto the NW layer or a transparent filling material such as spin-on-glass or an inert polymer can be used to reduce leakage current. Intrinsically-doped, n-type ZnO NWs have been grown on both, p-type or n-type Si substrates, where the dependence of the dark current on applied bias is found to resemble the ideal relationship for heterojunctions, with typical rectifying behavior:[37]

$$I = I_s\left[\exp\left(\frac{eV}{k_B T}\right) - 1\right] \tag{21}$$

where I_s is the saturation current and the other symbols have their usual meaning. In the case of the n-ZnO NW/p-Si heterojunction, photoconductivity studies performed under UV light illumination and reverse bias have shown responsivity of $\sim$0.07 A/W at -20 V applied bias,[106] with fast and slow components of the photocarrier dynamics of the order of $\sim$300 ms and few minutes, respectively.[108] Interestingly, in the case of n-ZnO NW/n-Si heterojunction, the spectral sensitivity could be tuned from the visible to the ultraviolet spectral regions by applying forward or reverse bias to the device, by controlling the band-offset at the heterointerface and by selectively collecting photocarriers that are generated in the Si substrate, or in the ZnO NWs, respectively.[109] Recent advances in the direct heteroepitaxial growth of III–V NWs on Si will also open up new opportunities for vertical NW array photodetectors and photovoltaics.[110–112]

One of the most interesting cases of NW photodetectors is given by avalanche photodiodes (APDs), where operation at large reverse bias allows each photogenerated carrier to be multiplied by avalanche breakdown caused by band-to-band carrier impact ionization. Carrier multiplication results in internal gain within the photodiode, which increases the effective responsivity of the device. The figure of merit for this process is the multiplication factor (or gain) M, which indicates the average number of carriers produced from the initial photocarriers:[113]

$$M = \frac{1-k}{e^{-\delta(1-k)} - k}, \quad k = \beta(E)/\alpha(E) \tag{22}$$

where δ is the average number of ionization events per electron transit, and α and β are the field-dependent ionization rates for electrons and for holes, respectively. So far, NW APDs have been demonstrated in two different configurations, namely a "crossed" n-CdS/p-Si NW heterojunction (Fig. 6(d)),[18] and an axial p-i-n single Si NW homojunction (Fig. 6(a)).[19] In the case of the n-CdS/p-Si "crossed" avalanche photodiode, a photocurrent increase (I_{PC}/I_{dark}) of $\sim 10^4$ times higher than in individual n-CdS or p-Si NW photoconductors has been observed due to avalanche multiplication at the p-n crossed NW junction, with multiplication factors as high as $M = 7\times10^4$. Polarization dependence of the photoresponse has also been observed in the "crossed" structure, due to the predominant optical absorption in the CdS NW, as verified by spectral measurements. A detection limit of about 75 photons was estimated for these devices.[18] Very similar results (namely polarization sensitivity, high spatial resolution, and high sensitivity) were obtained in the case of the axial p-i-n Si NW APD, where complementary doping within a single NW was used instead of the assembly of two distinctly doped NWs. A maximum multiplication factor of $M = 40$ was derived in this case. Interestingly, multiplication factors for electron and hole injections could also be isolated, indicating that the multiplication factor for electrons ($M_n < 100$) was larger than that for holes ($M_p < 20$) due to larger electron ionization rate ($\alpha > \beta$).[19]

3.1.2. Schottky Junctions

Metal-semiconductor junctions can be used as photodiodes where both, the electrons photoexcited in the metal and the electron–hole pairs photogenerated in the semiconductor can contribute to the photocurrent. One of the advantages of Schottky photodiodes is the fast response speed, due to the high electric field (thus the short carrier transit time) across the junction under reverse bias. The current in an ideal Schottky diode is still given by Eq. (21), with the reverse bias saturation current given by:[37]

$$I_s = A^* T^2 \exp\left(-\frac{e\phi_b}{kT}\right) \tag{23}$$

where A^* is Richardson's constant, and ϕ_b the Schottky barrier height. To account for the deviation from the ideal behavior, Eq. (21) is further modified as:[114]

$$I = I_s\left[\exp\left(\frac{e(V - V_{th})}{nk_B T}\right) - 1\right] \tag{24}$$

in which V_{th} is the forward-bias threshold voltage, and n the ideality factor. When the current is dominated by thermionic emission over the Schottky barrier $n = 1$.

The effects of Schottky barriers at the metal-semiconductor interface are often encountered in the literature of semiconductor NWs. In particular, scanning photocurrent microscopy (SPCM) has proven a valuable tool for the investigation of these effects in NW photodetectors. In SPCM experiments conducted on Si,[16] CdS,[58,115] and CdSe,[116] NWs, photocurrent–voltage characteristics were typically asymmetric and, depending on the biasing conditions, photocurrent could be strongly localized near the metal electrode-NW contact. This technique is very effective to investigate the mechanisms of photoconduction at the nanoscale, such as mapping the electronic band profile along the NW axis[16,116] or determining the carrier mobility-lifetime products.[58]

Despite the good understanding of metal-semiconductor junctions in NW devices, the intentional fabrication of Schottky photodiodes has been rarely pursued in materials other than ZnO NWs and nanobelts. Nobel metals such as Au, Ag and Pd tend to form Schottky contacts with n-ZnO, therefore two-terminal NW devices with symmetric contacts made of these metals usually behave as back-to-back Schottky diodes, and are responsive to UV illumination.[117–120] Ideality factors of ZnO NW Schottky photodiodes extracted by using Eq. (24) are often considerably larger than unity, due to the influence of both interface and surface states.[121,122] However, an almost ideal Pt/ZnO NW Schottky junction photodiode could also be demonstrated.[123] In this study, the I–V characteristic in the dark was well described by the thermionic emission model ((Eqs. (23) and (24)), and the diode had an excellent ideality factor of $n = 1.1$ at room temperature and very low reverse current. Interestingly, under UV illumination the device showed strong photoresponse, and the I–V characteristic became linear. The transition from rectifying to ohmic behavior was attributed to the lowering of the potential barrier between the Schottky contact and the ZnO NW under illumination. A similar behavior had been previously observed in a mesh of ZnO NWs contacted between two Au electrodes, where the transition from Schottky to ohmic behavior was observed exclusively upon illumination with photon energy above the ZnO bandgap.[124] The large difference in the photocurrent relaxation times observed in these two cases ($\tau < 33$ ms vs. $\tau > 10^4$) was ascribed to bulk-dominated rather than surface-dominated transport.

3.2. Phototransistors

A phototransistor is a bipolar or unipolar transistor where light can reach the base, creating optically generated carriers. This modulates the base-collector junction resulting in an amplified current through transistor action, which can lead to much greater photosensitivity. As discussed in the following, such structures have been successfully implemented in NW architectures. Typically, NW field-effect transistors have been fabricated dispersing NWs on a dielectric-semiconductor substrate.[17,48,70,76,88,125] or by patterning NWs through conventional lithographic methods.[45,46,126,127] Subsequently, a gate bias is applied through a lithographically patterned top gate, or a back gate. Sensitivity even down to a single charge carrier has been demonstrated using a double gated Si NW phototransistor.[127] This was achieved by a very narrow gate which acted as a trap for one carrier species. When light is illuminating the device, only a few carriers are trapped under the gate, and their recombination could be sensed through a sudden abrupt decrease in conductivity.

In the case of these field effect transistor photodetectors, an electrical gate bias is used to modulate the lateral field across the NW. However, a similar effect is also present in NW photoconductors in which surface states give rise to a radial electric field. As discussed in Section 2.4, this causes the separation of photogenerated carriers in the NW channel, which greatly extends the carrier recombination lifetime leading to a much higher sensitivity. Thus, NW photoconductors can be viewed as phototransistors where the internal field arising from the large density of surface states in conjunction with light illumination act as a photogate. Depending on the NW material, band bending can be caused by different surface mechanisms, such as the presence of a strong surface electric (as in GaN NWs)[28,32] or the presence of deep trap states (for instance oxygen-related hole traps in ZnO NWs or surface states in Ge NWs).[31,48] In order to clarify these points, we studied the photoconduction mechanism in Si NWs, finding that the phototransistive gain mechanism is also trap related.[25] In our experiments, p-type doped Si NW planar arrays fabricated by conventional photolithography and thermal oxidation (Fig. 7(a)) showed gain values of $G > 3.5 \times 10^4$ at low light intensities (Fig. 7(b)).

Due to the large number of surface states, the Si NWs in the dark are fully depleted of majority carriers, which are trapped at the surface. When light is absorbed by the NW, the minority carriers are swept to the surface where they recombine with the majority carriers. The remaining majority carriers continue to contribute to the photocurrent until they are captured at the surface. Thus we find that the gain of the device is governed by the majority carrier capture time rather than the minority carrier lifetime of photoconductors. Quantitatively, this can be described as follows. The average total current in a single NW detector considered as a two carrier system is given by:

$$\langle I \rangle = \frac{e\langle p_f \rangle}{\tau_h} + \frac{e\langle n \rangle}{\tau_t} \tag{25}$$

where $\langle I \rangle$ is the average total DC current (photocurrent and dark current), e is the electron charge, $\langle p_f \rangle$ and $\langle n \rangle$ are the average number of free holes and electrons in the

Delivered by Ingenta to: Nanyang Technological University IP: 155.69.4.4 Mon, 10 May 2010 07:45:18

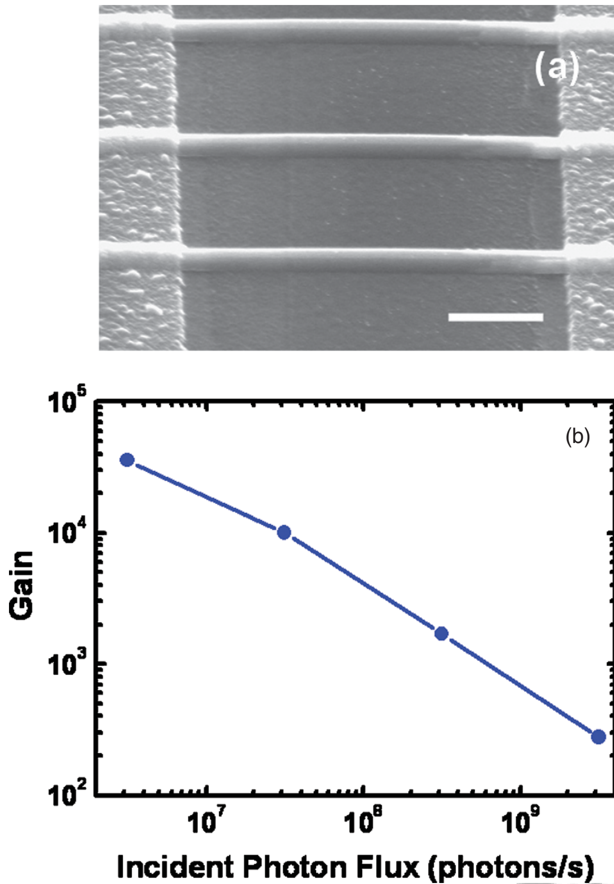

Fig. 7. (a) SEM image of a planar-etched Si NW array fabricated from a silicon-on-insulator wafer. The Scale bar is 2 μm. (b) Gain of a Si NW photodetector relative to the photon absorption rate extracted from photocurrent measurements at 0.5 V applied bias. Reprinted with permission from [25], A. Zhang et al., *Appl. Phys. Lett.* 93, 121110 **(2008)**. © 2008, American Institute of Physics.

NW respectively, and τ_h and τ_t are the hole and electron transit times respectively. We can also write the rate equations for the average free holes, electrons, and trapped holes, $\langle p_t \rangle$ including photogenerated carriers as:

$$\frac{d}{dt}\langle p_f \rangle = -\frac{\langle p_f \rangle}{\tau_c} + \frac{\langle p_t \rangle}{\tau_e} + \left[g_{\text{th}} + \eta^* \frac{P_{\text{opt}}}{\hbar\omega} \right] = -\frac{\langle p_f \rangle}{\tau_c} + \frac{\langle p_t \rangle}{\tau_e} + g_{\text{tot}} \tag{26}$$

$$\frac{d}{dt}\langle p_t \rangle = \frac{\langle p_f \rangle}{\tau_c} - \frac{\langle p_t \rangle}{\tau_e} - \frac{\langle n \rangle}{\tau_n} \tag{27}$$

$$\frac{d}{dt}\langle n \rangle = -\frac{\langle n \rangle}{\tau_n} + \left[g_{\text{th}} + \eta^* \frac{P_{\text{opt}}}{\hbar\omega} \right] = -\frac{\langle n \rangle}{\tau_n} + g_{\text{tot}} \tag{28}$$

Here τ_c, τ_e and τ_n are the average capture time for holes, escape time for holes, and capture time for electrons at the surface respectively, g_{th} is the thermal generation rate, $\eta^* P_{\text{opt}}/\hbar\omega$ is the photon absorption rate, and g_{tot} is the total carrier generation rate. In the case of Si NW phototransistors, we can neglect the escape of electrons from surface states, as any captured electron will immediately recombine with one of the large number of captured holes. This is reflected in Eq. (27) as a decrease of trapped holes due to electron capture. Let us first look at the DC current characteristics by finding the steady state solution to these equations when $d\langle p_f \rangle/dt = d\langle p_t \rangle/dt = d\langle n \rangle/dt = 0$. Solving for each carrier in Eqs. (26) and (27), and inserting into the total current Eq. (25),

$$I = \frac{e\tau_c \langle p_t \rangle}{\tau_h \tau_e} + \frac{e\tau_c g_{\text{tot}}}{\tau_h} + \frac{e\tau_n g_{\text{tot}}}{\tau_t} \approx \frac{e\tau_c}{\tau_h}\left(\frac{\langle p_t \rangle}{\tau_e} + g_{\text{tot}} \right) \tag{29}$$

assuming that the capture time for an electron is much faster than that for a hole ($\tau_n \ll \tau_c$) due to the large number of holes already trapped at the surface. Thus, the electron contribution to the current is negligible due to its fast trapping time. The first term $\langle p_t \rangle/\tau_e$ is the background contribution to the current due to trapped hole emission from surface states, which is related to the *p*-doping concentration in the NW while the second term g_{tot} is the contribution from thermal and photo generation in the NW. All these contributions experience a DC gain of $G_{\text{PT}} = \tau_c/\tau_h$. This phototransistive gain term is very similar to the photoconductive gain in Eq. (15), with the exception that now the majority carrier (hole) capture lifetime τ_c instead of the minority carrier recombination lifetime τ determines the photoconductive gain.

by Ingenta to: nological University 155.69.4.4 ay 2010 07:43:18 AMERICAN SCIENTIFIC PUBLISHERS

3.3. Superconductor Nanowire Photodetectors

Another photodetetector concept that makes use of the unique geometrical properties of NWs is that of superconducting NW photodetectors. So far, demonstrations of this concept have been focused on NbN NWs (with typical dimensions of ~5 nm thickness and 50–200 nm width), which ultimately yield single photon sensitivity with GHz counting rate and high detection efficiency.[128–133] Research is also undergoing to identify other suitable supeconducting materials, such as MoRe.[134] The working principles of superconducting NW detectors relies on the fact that the superconducting energy gap of a superconductor (2Δ) is two to three orders of magnitude lower than in a semiconductor, thus photon absorption in a superconducting detector creates an avalanche electron charge two to three orders of magnitude higher for the same photon energy. The absorption of a photon with energy $\hbar\omega \gg 2\Delta$ creates a local nonequilibrium perturbation with a large number of excited hot electrons, which increases the average electron temperature above T_c and results in the formation of a hotspot—a local nonsuperconducting region. The size of the resistive region grows as hot electrons diffuse out of the hotspot, and a non-superconducting barrier is formed across the entire width of the device (hence the need for NW geometry with narrow width). Ultimately, this results in a photosensitive *I–V* characteristic.[128] Since the energy relaxation time constants of excited electrons in superconductors are of the order of picoseconds, single photon

counters with GHz repetition rate are achievable by this method,[128, 129, 133] whose operation can extend from the visible to the infrared spectral region.[134, 135] After the addition of an optical cavity and an anti-reflection coating, detection efficiencies as high as 67% and 57% were obtained at wavelengths of 1064 and 1550 nm, respectively.[130]

3.4. Metal and Metal-Dielectric Nanowire Photodetectors

Another unconventional NW photodetector concept makes use of metallic NWs with diameters of few nanometers. Giant photoconductive increase ($\sim$100) has been observed in Au NWs with small restrictions when illuminated by light pulses,[136] an effect that would be totally unexpected in metals. Moreover, the conductance in these systems was found to increase by quantized increments upon pulsed illumination, with rise and relaxation times after photoexcitation of the order of milliseconds. Although the origin of these observations is not completely understood, they were tentatively attributed to an increase in NW diameter under illumination due to local heating. Large diameter metallic NWs, in which the conductance is still quantized, can accommodate a larger number of modes and thus sustain larger currents. Recently, photoinduced voltage has also been observed in macroscopic bundles of Ag core/Ni shell NW heterojunctions.[137] This type of NW photodetector schemes may prove useful in conjunction with plasmonic elements for nanophotonic applications. Metal-dielectric NWs, such as "peapod" systems in which metal nanoparticles are embedded in dielectric NWs can also be utilized for light sensing applications. For example, Au nanoparticle embedded in silica NWs have shown large photoresponse at photon energies resonant with surface plasmon polaritons.[138]

Delivered by Ingenta to:
Nanyang Technological University
IP : 155.69.4.4
Mon, 10 May 2010 07:45:18

4. NANOWIRE POTODETECTOR APPLICATIONS

So far we have described how NWs are utilized as building blocks for different photodetector concepts, and how their geometrical, material, and low-dimensional properties allow achieving unique sensitivity and functionalities. In the following we will present some applications that we have identified, in which NW photodetector may offer unique advantages over their thin-film or bulk counterparts, namely optical intrachip interconnects, single-photon detectors, and image sensors.

4.1. Optical Intrachip Interconnects

The extremely large internal gain achievable in NW photodetectors could be exploited for emerging applications such as optical intrachip interconnects. To minimize clock skew, electrical impedance mismatch, and switching energy-per-bit for multi-core processors, it is paramount to achieve high-sensitivity on-chip photoreceivers that consume minimal power.[139] For example, assuming a capacitive load of 10 fF, the energy-per-bit for intrachip interconnect would be 10 fJ/bit. This number suggests that it will take 6×10^4 electrons to charge up the capacitor to 1 V. To achieve a data rate of 10 Gb/s with a PIN diode with 60% quantum efficiency and operating wavelength of 1550 nm, the detector would need to be irradiated with 10^5 photons in 100 ps. This corresponds to a sensitivity of about -10 dBm or 0.1 mW optical power, which is nearly 10 dB worse than the state-of-the-art telecom 10 Gb/s PIN-FET receivers and 17 dB worse than the APD receivers. However, these are not practical for intrachip interconnects due to the high power consumption required for amplification or the high operating voltage. With a low mobility material such as ZnO with 2 μm electrode spacing, we have measured a *GB* product of 3–6 GHz,[31] and sub-nanosecond photocurrent relaxation times have been shown.[31, 140] For high mobility NWs such as InGaAs and Ge with a shorter electrode spacing (0.2 μm), the carrier transit time would reach sub-picoseconds, and the *GB* product 500 GHz to 1 THz. At 10 Gb/s operation, NW photodetectors could then allow achieving gain of 50–100, yielding -25 to -30 dBm receiver sensitivity, which is commensurate with the state-of-the-art APD receivers but at a lower operating voltage of <1 V. NW photodetectors with extremely high internal gain and gain bandwidth product are therefore very attractive to achieve amplifier-free, high sensitivity receivers and save power consumption and real estate of postamplifiers in optical intrachip interconnects. In addition, NW detectors can reduce thermal noise and, at the same gain and current level, operate at a much lower voltage than avalanche photodetectors.

AMERICAN
SCIENTIFIC
PUBLISHERS

4.2. Single-Photon Detectors

The extremely large photosensitivity of NWs could ultimately enable single-photon detection. As discussed in Section 3, sensitivity of $\sim$75 photons has been already demonstrated in NW APDs at room temperature,[18] and single-photon sensitivity was achieved in superconductor NWs operated at $T < 4.2$ K.[129–135] In the following we will evaluate the possibility of achieving single-photon response in NW photoconductors, considering the p-Si NW phototransistor described in Section 3.2 as a model system. In this case, the transient response due to a single carrier generation can be derived by solving the following system of coupled rate equations, where an impulse term is added to the free hole and electron generation rates:

$$\frac{d}{dt}\langle p_f \rangle = -\frac{\langle p_f \rangle}{\tau_c} + \frac{\langle p_t \rangle}{\tau_e} + g_{\text{tot}} + \delta(t) \qquad (30)$$

$$\frac{d}{dt}\langle p_t \rangle = \frac{\langle p_f \rangle}{\tau_c} - \frac{\langle p_t \rangle}{\tau_e} - \frac{\langle n \rangle}{\tau_n} \qquad (31)$$

$$\frac{d}{dt}\langle n\rangle = -\frac{\langle n\rangle}{\tau_n} + g_{\text{tot}} + \delta(t) \tag{32}$$

To solve these coupled differential equations, one can take the Laplace transform to linearize the system, and solve for $P_f(s)$, $P_t(s)$, and $N(s)$ with the assumptions that, in the frequencies of interest, electron trapping is fast (i.e., $|\tau_n s| \ll 1$), hole emission is slow (i.e., $|\tau_e s| \gg 1$), and the number of trapped holes is much larger than the number of electrons (i.e., $P_t(0) \gg N(0)$ and $P_t(0) \gg 1$). After taking the inverse transform, the transient behavior resulting from the impulse response is:

$$\langle p_t(t)\rangle \approx \langle p_t(0)\rangle \tag{33}$$

$$\langle p_f(t)\rangle \approx \langle p_f(0)\rangle + e^{-t/\tau_c} \tag{34}$$

Here we have neglected the $n(t)$ term as we are interested in the current produced by the single carrier generation, and the electrons have a negligible contribution due to their fast trapping time. From Eq. (33), it is seen that the number of trapped holes does not significantly change upon a single carrier photogeneration event. This is reasonable considering the large number of holes already trapped at the surface. Thus, the change in current due to the single carrier generation would be:

$$\langle \Delta I(t)\rangle = \frac{e}{\tau_h}(\langle p_f(t)\rangle - \langle p_f(0)\rangle) = \frac{e}{\tau_h} e^{-t/\tau_c} \tag{35}$$

As a result of a single carrier generation in the NW, the instantaneous current change shows an exponential decay with a lifetime of the average capture time constant of holes. This plays an important role in actual measurement of such a response, where current is averaged over the integration time T. Therefore the measured current becomes:

$$\langle \Delta I\rangle = \frac{e}{\tau_h}\frac{\int_0^T e^{-t/\tau_c}\,dt}{T} = \frac{e\tau_c}{\tau_h T}(1 - e^{-T/\tau_c}) \approx \begin{cases} \dfrac{e\tau_c}{\tau_h T} & \text{for } T \gg \tau_c \\[2ex] \dfrac{e}{\tau_h} & \text{for } T \ll \tau_c \end{cases} \tag{36}$$

For sampling times much longer than the hole capture time, the current increase due to a single photocarrier generation event is greatly reduced. To observe single photon response, the signal to noise ratio (S/N) must be greater than one. The noise of the photocurrent is dominated by generation-recombination noise and can therefore be written as:

$$\langle I^2\rangle = \frac{2eIB(\tau_c/\tau_h)}{1 + (2\pi B\tau_c)^2} + 2elB \approx \frac{2elB(\tau_c/\tau_h)}{1 + (2\pi B\tau_c)^2} \tag{37}$$

Here $B = 1/2T$ is the bandwidth of the measuring system. We have assumed that the excess noise from gain fluctuation and the thermal noise are negligible due to the high impedance of our device, and the shot noise is small compared to the generation-recombination noise. Notice that the coefficient for the generation-recombination noise term has been modified from the usual value of 4 in a two carrier system to a value of 2 since in our device only the majority carriers contribute to the current, and therefore to the noise. The signal to noise ratio for single-photon detection under the condition $T \ll \tau_c$ can be obtained using Eqs. (25) and (34–37), and the approximation $\langle n\rangle \ll \langle P_f\rangle \ll 1$:

$$\frac{S}{N} = \frac{\langle \Delta I\rangle^2}{\langle I^2\rangle} \approx (1 - e^{-T/\tau_c})\left[1 + \left(\frac{\pi\tau_c}{T}\right)^2\right] \tag{38}$$

The approximation in Eq. (38) holds when the nanowire detector is depleted $\langle P_f\rangle \ll 1$. Nanowire depletion is a particularly important requirement for single-photon detection, otherwise the signal to noise ratio can fall well below unity. Single photon resolution is therefore achievable in theory, provided that the integration time T is comparable to the hole capture time τ_c. From Eq. (37), the maximum signal to noise ratio for single photon response is about 7 when $T \sim \tau_c$. For Si nanowire detectors fabricated in our laboratories, we have a hole transit time of $\tau_h \approx 5.7$ ns, and a hole capture time of $\tau_c \approx 200\ \mu$s, as estimated from the value of gain ($G_{\text{PT}} \sim 3.5 \times 10^4$). This leads to the maximal single-photon sensitivity at around 2.5 KHz, provided the predominant noise is generation-recombination noise represented by Eq. (37).

4.3. Image Sensors

The large photosensitivity of NWs combined with their potential for dense spatial integration make them also interesting for image sensors based on new concepts.[141] Any of the NW photodetector architectures described above could be in principle utilized to this end, provided that NWs could be consistently organized in ordered arrays and selectively addressed. Hence, the major challenge for the advancement of this technology is the precise positioning of NWs in desired locations and their integration with the pixel driving circuitry on a large scale. Besides direct patterned NW growth,[142] other techniques that can be used to transfer NWs with controlled positioning and alignment on host substrates include the Langmuir Blodgett method,[143, 144] dielectrophoresis,[59, 75, 120, 121, 145] microfluidic alignment,[18] the "bubble-blow" technique,[146] dry transfer (or contact printing),[147–149] and possibly ink-jet printing.

The first 1×16 NW photodetector array for imaging applications has been demonstrated by making use of conventional top-down CMOS fabrication technology combined with photo and electron-beam lithography and thermal oxidation steps. Thanks to the high responsivity of the NW photodetectors ($>1 \times 10^2$ A/W),

Delivered by Ingenta to: Nanyang Technological University IP: 155.69.4.4 Mon, 10 May 2010 07:45:18 AMERICAN SCIENTIFIC PUBLISHERS

image acquisition capabilities at low-illumination conditions could be demonstrated with this device.[150]

Alternative NW image sensor concepts, in which heterogeneous circuitry is formed either before or after transferring the NWs from the growth to the host substrate are rapidly developing. The main advantage of these schemes is allowing integration of NWs of different materials, thus allowing various combinations of spectral sensitivity (e.g., for UV, VIS or IR image sensors that are blind to unwanted photon energies, or RGB discrimination for color imaging) and optoelectronic properties (e.g., integration of high-mobility III–V compound semiconductors on Si). Preliminary demonstrations of heterogeneous NW arrays for imaging applications have been reported.[18,149] As presented in Section 3.2, NW avalanche photodiodes made by the assembly of "crossed" heterojunctions have shown sub-wavelength spatial sensitivity (<250 nm) and ultra-high sensitivity (~100 photons). Moreover, an array of two "crossed" NW APD has also been realized by microfluidic alignment, showing that the two pixels could be addressed independently and without cross-talk.[18] A major step forward has been recently made by the demonstration of a relatively large (13×20) NW image sensor array by a combination of contact NW transfer and standard photolithographic techniques. In this work, CdSe single NWs or NW arrays were used as highly sensitive photoactive elements, while high-mobility core–shell Ge/Si NWs were used to assemble active FET amplifiers. A contrast map of a focused light beam was obtained from the 13×20 array of NW-based active pixels, clearly demonstrating the potential of these NW circuit matrix for image sensing applications.[149]

Delivered by Inge
Nanyang Technologica
IP : 155.69.4
Mon, 10 May 2010
AMERICAN SCIENTIFIC PUBLISHERS

In view of realizing large-scale, ordered NW photodetector arrays, in which the absorption properties can be tailored by design (see Section 2.2), nanoimprint lithography (NIL) is one of the most promising methods since it can reduce both processing time and cost while granting nanometer-scale feature resolution and high yield. NIL can be employed for the fabrication of vertical NW photodetector arrays, either via the top-down (etching) method or the bottom-up (metal catalyzed or selective area) chemical NW synthesis.[151,152] The process involves physically pressing a mold (usually defined by electron-beam lithography), with the pattern to be imprinted, onto a resist. This creates a three-dimensional topography of the pattern in the resist. The resist is then cured by either UV or thermal methods and, once separated from the mold, etched until the thinner regions are completely removed. An example of the etch-mask and Si NW array obtained in our laboratories by the NIL method is shown in Figure 8. Experiments to integrate these NW arrays into functional circuits in which NWs are addressed individually are undergoing. Being also compatible with standard CMOS processing, we believe this technology holds great potential.

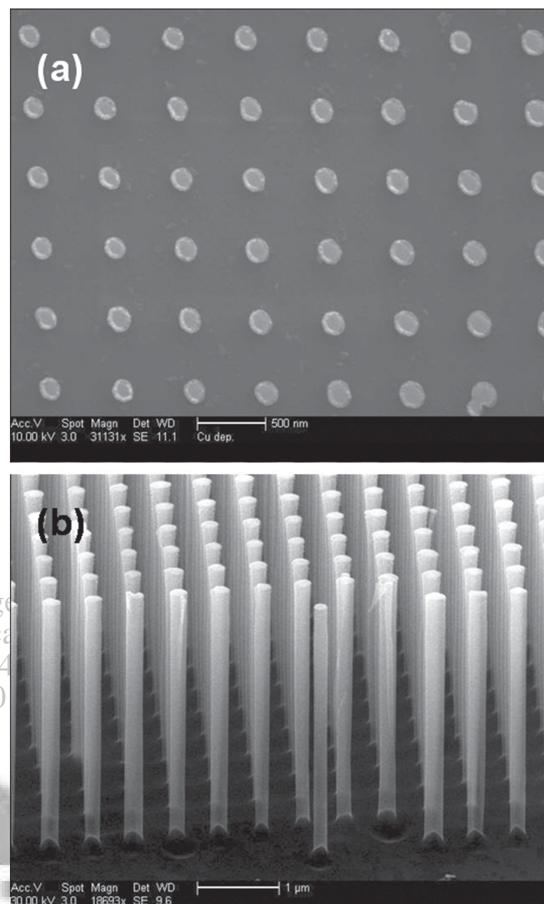

Fig. 8. (a) SEM image of the etch-mask obtained by patterning 60 nm thick Ni discs on a Si substrate by NIL. The Ni disc diameter and pitch are 180 and 500 nm, respectively. (b) Si NW array obtained by reactive-ion-etching of the etch-mask in (a).

5. SUMMARY AND CONCLUSIONS

In summary, we have given a broad overview on different NW photodetector concepts and their possible applications. We have shown that, from simple NW photoconducting devices to more complicated NW photodetector architectures, one-dimensional or quasi-one-dimensional nanostructures offer several advantages over their bulk or thin-film counterparts, specifically:

(i) Dense device integration and sub-wavelength spatial resolution;

(ii) Reduced optical losses due to enhanced light scattering and enhanced light absorption in vertical NW arrays;

(iii) Discrimination of light polarization;

(iv) Large photosensitivity due to internal photoconductive or phototransistive gain;

(v) Possibility to integrate functionality within single NW devices (e.g., photodiodes, APDs etc.);

(vi) Heterogeneous integration of NWs and substrates of different materials for enhanced or specific spectral sensitivity;

(vii) Possibility to develop novel photodetector concepts based on one-dimensional effects (e.g., superconductor and metallic NW photodetectors).

Although this review does not claim to be exhaustive of the entire literature related to NW photodetectors (we apologize for those articles that we may have inadvertently omitted), we hope it could give a sense of the substantial body of work that was done in this field. We believe that NW photodetectors are extremely interesting from both, a fundamental and a technological perspective. From the scientific point of view, NW photodetector research is highly interdisciplinary, and involves the physics of low-dimensional nanostructures, materials science, and device engineering. From the practical point of view, NW photodetectors are becoming a mature technology, and we foresee their emergence in applications for light detection and imaging, signal processing, and biological or chemical photometric sensing.

Acknowledgments: The authors acknowledge the technical support of the staff of the Nano3 Facility where the NW detectors were fabricated. This work was partially supported by the Office of Naval Research (ONR-nanoelectronics), the National Science Foundation (ECS-0506902), Sharp Labs of America, and by DHS and DOE SBIR grants from Agiltron Incorporated. Arthur Zhang acknowledges support from a National Science Foundation Graduate Research Fellowship.

References and Notes

1. C. Thelander, P. Agarwal, S. Brongersma, J. Eymery, L. F. Feiner, A. Forchel, M. Scheffler, W. Riess, B. J. Ohlsson, U. Gosele, and L. Samuelson, *Mater. Today* 9, 28 **(2006)**.
2. Y. Li, F. Qian, J. Xiang, and C. M. Lieber, *Mater. Today* 9, 18 **(2006)**.
3. P. J. Pauzauskie and P. Yang, *Mater. Today* 9, 36 **(2006)**.
4. R. H. Bube, Photoconductivity of Solids, Wiley, New York **(1960)**.
5. A. Rose, Concepts in Photoconductivity and Allied Problems, Interscience Publishers, New York **(1963)**.
6. R. H. Bube, Photoelectronic Properties of Semiconductors, Cambridge University Press, Cambridge, New York **(1992)**.
7. H. E. Ruda and A. Shik, *Phys. Rev. B* 72, 115308 **(2005)**.
8. H. E. Ruda and A. Shik, *J. Appl. Phys.* 100, 024314 **(2006)**.
9. J. Qi, A. M. Belcher, and J. M. White, *Appl. Phys. Lett.* 82, 2616 **(2003)**.
10. Z. H. Zhang, X. Y. Qi, J. K. Han, and X. F. Duan, *Micron* 37, 229 **(2006)**.
11. C. S. Peter and J. V. Kerry, *Appl. Phys. Lett.* 57, 545 **(1990)**.
12. Z. Xinyuan, C. M. Wei, L. Yang, and M. Y. Chou, *Phys. Rev. Lett.* 92, 236805 **(2004)**.
13. H. E. Ruda and A. Shik, *Proceedings of SPIE-The International Society for Optical Engineering* 6099, 60990L1 **(2006)**.
14. J. F. Wang, M. S. Gudiksen, X. F. Duan, Y. Cui, and C. M. Lieber, *Science* 293, 1455 **(2001)**.
15. Z. Y. Fan, P. C. Chang, J. G. Lu, E. C. Walter, R. M. Penner, C. H. Lin, and H. P. Lee, *Appl. Phys. Lett.* 85, 6128 **(2004)**.
16. Y. Ahn, J. Dunning, and J. Park, *Nano Lett.* 5, 1367 **(2005)**.
17. S. Han, W. Jin, D. H. Zhang, T. Tang, C. Li, X. L. Liu, Z. Q. Liu, B. Lei, and C. W. Zhou, *Chem. Phys. Lett.* 389, 176 **(2004)**.
18. O. Hayden, R. Agarwal, and C. M. Lieber, *Nat. Mater.* 5, 352 **(2006)**.
19. C. Yang, C. J. Barrelet, F. Capasso, and C. M. Lieber, *Nano Lett.* 6, 2929 **(2006)**.
20. H. Pettersson, J. Tragardh, A. I. Persson, L. Landin, D. Hessman, and L. Samuelson, *Nano Lett.* 6, 229 **(2006)**.
21. A. Singh, X. Li, V. Protasenko, G. Galantai, M. Kuno, H. Xing, and D. Jena, *Nano Lett.* 7, 2999 **(2007)**.
22. Y. H. Yu, V. Protasenko, D. Jena, H. L. Xing, and M. Kuno, *Nano Lett.* 8, 1352 **(2008)**.
23. O. L. Muskens, M. T. Borgstrom, E. P. A. M. Bakkers, and J. G. Rivas, *Appl. Phys. Lett.* 89, 233117 **(2006)**.
24. L. Hu and G. Chen, *Nano Lett.* 7, 3249 **(2007)**.
25. A. Zhang, S. You, C. Soci, Y. Liu, D. Wang, and Y.-H. Lo, *Appl. Phys. Lett.* 93, 121110 **(2008)**.
26. O. L. Muskens, J. G. M. Rivas, R. E. Algra, E. P. A. M. Bakkers, and A. Lagendijk, *Nano Lett.* 8, 2638 **(2008)**.
27. F. Szmulowicz and T. C. Chandler, *IEEE Transactions on Electron Devices* 28, 772 **(1981)**.
28. R. Calarco, M. Marso, T. Richter, A. I. Aykanat, R. Meijers, A. V. Hart, T. Stoica, and H. Luth, *Nano Lett.* 5, 981 **(2005)**.
29. L. Wang and P. Asbeck, *Sixth IEEE Conference on Nanotechnology* **(2006)**, Vol. 2, p. 716.
30. J. S. Jie, W. J. Zhang, Y. Jiang, X. M. Meng, Y. Q. Li, and S. T. Lee, *Nano Lett.* 6, 1887 **(2006)**.
31. C. Soci, A. Zhang, B. Xiang, S. A. Dayeh, D. P. R. Aplin, J. Park, X. Y. Bao, Y. H. Lo, and D. Wang, *Nano Lett.* 7, 1003 **(2007)**.
32. C. Reui-San, C. Hsin-Yi, L. Chien-Yao, C. Kuei-Hsien, C. Chin-Pei, C. Li-Chyong, and Y. Ying-Jay, *Appl. Phys. Lett.* 91, 223106 **(2007)**.
33. J. D. Prades, R. Jimenez-Diaz, F. Hernandez-Ramirez, L. Fernandez-Romero, T. Andreu, A. Cirera, A. Romano-Rodriguez, A. Cornet, J. R. Morante, S. Barth, and S. Mathur, *J. Phys. Chem. C* 112, 14639 **(2008)**.
34. J. D. Prades, F. Hernandez-Ramirez, R. Jimenez-Diaz, M. Manzanares, T. Andreu, A. Cirera, A. Romano-Rodriguez, and J. R. Morante, *Nanotechnology* 19, 465501 **(2008)**.
35. S. Mathur, S. Barth, H. Shen, J. C. Pyun, and U. Werner, *Small* 1, 713 **(2005)**.
36. F. Stockmann, *Appl. Phys.* 7, 1 **(1975)**.
37. S. M. Sze, Physics of Semiconductor Devices, Wiley, New York **(1981)**.
38. T. Takahashi, K. Takada, and M. Takeuchi, *Ultramicroscopy* 97, 1 **(2003)**.
39. D. Cooke, Z. Wu, X. Mei, J. Liu, H. E. Ruda, K. L. Kavanagh, and F. A. Hegmann, *American Physical Society, March Meeting 2004*, Palais des Congres de Montreal, Montreal, Quebec, Canada **(2004)**.
40. D. G. Cooke, F. A. Hegmann, I. M. Yu, M. W. Zh, W. Black, H. Wen, G. J. Salamo, T. D. Mishima, G. D. Lian, and M. B. Johnson, *J. Appl. Phys.* 103, 023710 **(2008)**.
41. V. J. Logeeswaran, A. Sarkar, M. S. Islam, N. P. Kobayashi, J. Straznicky, X. Li, W. Wu, S. Mathai, M. R. T. Tan, S. Y. Wang, and R. S. Williams, *Applied Physics a-Materials Science & Processing* 91, 1 **(2008)**.
42. M. Kang, J. S. Lee, S. K. Sim, H. Kim, B. Min, K. Cho, G. T. Kim, M. Y. Sung, S. Kim, and H. S. Han, *Jpn. J. Appl. Phys., Part 1* 43, 6868 **(2004)**.
43. P. Servati, A. Colli, S. Hofmann, Y. Q. Fu, P. Beecher, Z. A. K. Durrani, A. C. Ferrari, A. J. Flewitt, J. Robertson, and W. I. Milne, *Physica E: Low-dimensional Systems and Nanostructures* 38, 64 **(2007)**.
44. K. H. Kim, K. Keem, D. Y. Jeong, B. D. Min, K. A. Cho, H. Kim, B. Moon, T. Noh, J. Park, M. Suh, and S. Kim, *Jpn. J. Appl. Phys., Part 1* 45, 4265 **(2006)**.
45. H. G. Choi, Y. S. Choi, Y. C. Jo, and H. Kim, *Jpn. J. Appl. Phys., Part 1* 43, 3916 **(2004)**.

Delivered by Ingenta to: Nanyang Technological University IP: 155.69.4... Mon, 10 May 2010 07:43:18 AMERICAN SCIENTIFIC PUBLISHERS

46. J.-H. Park, H. Kim, I.-S. Wang, and J.-K. Shin, *Forth IEEE Conference on Nanotechnology* **(2004)**, p. 425.
47. B. Polyakov, B. Daly, J. Prikulis, V. Lisauskas, B. Vengalis, M. A. Morris, J. D. Holmes, and D. Erts, *Adv. Mater.* 18, 1812 **(2006)**.
48. Y. H. Ahn and P. Jiwoong, *Appl. Phys. Lett.* 91, 162102 **(2007)**.
49. W. Smith, *Nature* 7, 303 **(1873)**.
50. B. Gates, B. Mayers, B. Cattle, and Y. N. Xia, *Adv. Funct. Mater.* 12, 219 **(2002)**.
51. Y. Wang, Z. Y. Tang, P. Podsiadlo, Y. Elkasabi, J. Lahann, and N. A. Kotov, *Adv. Mater.* 18, 518 **(2006)**.
52. N. Kouklin, L. Menon, A. Z. Wong, D. W. Thompson, J. A. Woollam, P. F. Williams, and S. Bandyopadhyay, *Appl. Phys. Lett.* 79, 4423 **(2001)**.
53. Q. G. Li and R. M. Penner, *Nano Lett.* 5, 1720 **(2005)**.
54. T. Gao, Q. H. Li, and T. H. Wang, *Appl. Phys. Lett.* 86, 173105 **(2005)**.
55. Y. Gu and L. J. Lauhon, *Appl. Phys. Lett.* 89, 143102 **(2006)**.
56. Q. H. Li, T. Gao, and T. H. Wang, *Appl. Phys. Lett.* 86, 193109 **(2005)**.
57. Y. Gu, J. P. Romankiewicz, J. K. David, J. L. Lensch, and L. J. Lauhon, *Nano Lett.* 6, 948 **(2006)**.
58. Y. Gu, J. P. Romankiewicz, J. K. David, J. L. Lensch, L. J. Lauhon, E. S. Kwak, and T. W. Odom, *J. Vac. Sci. Technol., B* 24, 2172 **(2006)**.
59. R. H. Zhou, H. C. Chang, V. Protasenko, M. Kuno, A. K. Singh, D. Jena, and H. Xing, *J. Appl. Phys.* 101, 073704 **(2007)**.
60. D. J. Pena, J. K. N. Mbindyo, A. J. Carado, T. E. Mallouk, C. D. Keating, B. Razavi, and T. S. Mayer, *J. Phys. Chem. B* 106, 7458 **(2002)**.
61. J. Salfi, U. Philipose, C. F. de Sousa, S. Aouba, and H. E. Ruda, *Appl. Phys. Lett.* 89, 261112 **(2006)**.
62. U. Philipose, H. E. Ruda, A. Shik, C. F. de Souza, and P. Sun, *J. Appl. Phys.* 99, 066106 **(2006)**.
63. J. G. Lu, Z. Fan, D. Wang, and P.-C. Chang, *Proceedings of SPIE-The International Society for Optical Engineering* 5648, 260 **(2005)**.
64. K. Keem, J. Kang, D. Y. Jeong, B. Min, K. Cho, H. Kim, S. Kim, and Y. K. Kim, *Jpn. J. Appl. Phys., Part 1* 46, 4355 **(2007)**.
65. S. H. Lee, H. J. Lee, D. Oh, S. W. Lee, H. Goto, R. Buckmaster, T. Yasukawa, T. Matsue, S. K. Hong, H. Ko, M. W. Cho, and T. F. Yao, *J. Phys. Chem. B* 110, 3856 **(2006)**.
66. H. Kind, H. Q. Yan, B. Messer, M. Law, and P. D. Yang, *Adv. Mater.* 14, 158 **(2002)**.
67. Y. W. Heo, B. S. Kang, L. C. Tien, D. P. Norton, F. Ren, J. R. La Roche, and S. J. Pearton, *Applied Physics a-Materials Science & Processing* 80, 497 **(2005)**.
68. Q. H. Li, T. Gao, Y. G. Wang, and T. H. Wang, *Appl. Phys. Lett.* 86, 123117 **(2005)**.
69. Q. H. Li, Q. Wan, Y. X. Liang, and T. H. Wang, *Appl. Phys. Lett.* 84, 4556 **(2004)**.
70. Q. H. Li, Y. X. Liang, Q. Wan, and T. H. Wang, *Appl. Phys. Lett.* 85, 6389 **(2004)**.
71. H. Kind, H. Yan, B. Messer, M. Law, and P. Yang, *Adv. Mater. (Weinheim, Germany)* 14, 158 **(2002)**.
72. S. Kumar, V. Gupta, and K. Sreenivas, *Nanotechnology* 16, 1167 **(2005)**.
73. J. B. K. Law and J. T. L. Thong, *Appl. Phys. Lett.* 88, 133114 **(2006)**.
74. S.-E. Ahn, H. J. Ji, K. Kim, G. T. Kim, C. H. Bae, S. M. Park, Y.-K. Kim, and J. S. Ha, *Appl. Phys. Lett.* 90, 153106 **(2007)**.
75. J. Suehiro, N. Nakagawa, S. Hidaka, M. Ueda, K. Imasaka, M. Higashihata, T. Okada, and M. Hara, *Nanotechnology* 17, 2567 **(2006)**.
76. M. S. Arnold, P. Avouris, Z. W. Pan, and Z. L. Wang, *J. Phys. Chem. B* 107, 659 **(2003)**.
77. R. Ghosh, M. Dutta, and D. Basak, *Appl. Phys. Lett.* 91, 073108 **(2007)**.
78. M.-C. Jeong, B.-Y. Oh, W. Lee, and J.-M. Myoung, *Appl. Phys. Lett.* 86, 103105 **(2005)**.
79. C.-L. Hsu, S.-J. Chang, Y.-R. Lin, P.-C. Li, T.-S. Lin, S.-Y. Tsai, T.-H. Lu, and I. C. Chen, *Chem. Phys. Lett.* 416, 75 **(2005)**.
80. C. Y. Lu, S. J. Chang, S. P. Chang, C. T. Lee, C. F. Kuo, H. M. Chang, Y. Z. Chiou, C. L. Hsu, and I. C. Chen, *Appl. Phys. Lett.* 89, 153101 **(2006)**.
81. D. Park and K. Yong, *J. Vac. Sci. Technol., B* 26, 1933 **(2008)**.
82. S. H. Lee, H. J. Lee, D. Oh, S. W. Lee, H. Goto, R. Buckmaster, T. Yasukawa, T. Matsue, S.-K. Hong, H. Ko, M.-W. Cho, and T. Yao, *J. Phys. Chem. B* 110, 3856 **(2006)**.
83. Z. Y. Fan, D. Dutta, C. J. Chien, H. Y. Chen, E. C. Brown, P. C. Chang, and J. G. Lu, *Appl. Phys. Lett.* 89, 213110 **(2006)**.
84. P. Feng, J. Y. Zhang, Q. H. Li, and T. H. Wang, *Appl. Phys. Lett.* 88, 153107 **(2006)**.
85. P. Feng, J. Y. Zhang, Q. Wan, and T. H. Wang, *J. Appl. Phys.* 102, 074309 **(2007)**.
86. Z. Q. Liu, D. H. Zhang, S. Han, C. Li, T. Tang, W. Jin, X. L. Liu, B. Lei, and C. W. Zhou, *Adv. Mater.* 15, 1754 **(2003)**.
87. J. S. Lee, S. K. Sim, B. Min, K. Cho, S. W. Kim, and S. Kim, *J. Cryst. Growth* 267, 145 **(2004)**.
88. D. Zhang, C. Li, S. Han, X. Liu, T. Tang, W. Jin, and C. Zhou, *Applied Physics a-Materials Science & Processing* 77, 163 **(2003)**.
89. X. Liu, C. Li, S. Han, J. Han, and C. W. Zhou, *Appl. Phys. Lett.* 82, 1950 **(2003)**.
90. J. Park, E. Lee, K. W. Lee, and C. E. Lee, *Appl. Phys. Lett.* 89, 183114 **(2006)**.
91. D. Wang, F. Qian, C. Yang, Z. H. Zhong, and C. M. Lieber, *Nano Lett.* 4, 871 **(2004)**.
92. R. Agarwal, *Small* 4, 1872 **(2008)**.
93. A. Ambroziak, Semiconductor Photolectric Devices: An Introduction to Design, Iliffe, London **(1968)**.
94. B. M. Kayes, H. A. Atwater, and N. S. Lewis, *J. Appl. Phys.* 97, 114302 **(2005)**.
95. Y. Zhang, L.-W. Wang, and A. Mascarenhas, *Nano Lett.* 7, 1264 **(2007)**.
96. B. Tian, T. J. Kempa, and C. M. Lieber, *Chem. Soc. Rev.* 38, 16 **(2009)**.
97. M. D. Kelzenberg, D. B. Turner-Evans, B. M. Kayes, M. A. Filler, M. C. Putnam, N. S. Lewis, and H. A. Atwater, *Nano Lett.* 8, 710 **(2008)**.
98. T. J. Kempa, B. Z. Tian, D. R. Kim, J. S. Hu, X. L. Zheng, and C. M. Lieber, *Nano Lett.* 8, 3456 **(2008)**.
99. B. Z. Tian, X. L. Zheng, T. J. Kempa, Y. Fang, N. F. Yu, G. H. Yu, J. L. Huang, and C. M. Lieber, *Nature* 449, 885 **(2007)**.
100. K. Q. Peng, Y. Xu, Y. Wu, Y. J. Yan, S. T. Lee, and J. Zhu, *Small* 1, 1062 **(2005)**.
101. L. Tsakalakos, J. Balch, J. Fronheiser, B. A. Korevaar, O. Sulima, and J. Rand, *Appl. Phys. Lett.* 91, 233117 **(2007)**.
102. Y. B. Tang, Z. H. Chen, H. S. Song, C. S. Lee, H. T. Cong, H. M. Cheng, W. J. Zhang, I. Bello, and S. T. Lee, *Nano Lett.* 8, 4191 **(2008)**.
103. J. A. Czaban, D. A. Thompson, and R. R. LaPierre, *Nano Lett.* 9, 148 **(2009)**.
104. K. Wang, J. J. Chen, W. L. Zhou, Y. Zhang, Y. F. Yan, J. Pern, and A. Mascarenhas, *Adv. Mater.* 20, 3248 **(2008)**.
105. M. S. Son, S. I. Im, Y. S. Park, C. M. Park, T. W. Kang, and K. H. Yoo, *Materials Science & Engineering C-Biomimetic and Supramolecular Systems* 26, 886 **(2006)**.
106. L. Luo, Y. F. Zhang, S. S. Mao, and L. W. Lin, *Sensors and Actuators a-Physical* 127, 201 **(2006)**.
107. J. H. He, S. T. Ho, T. B. Wu, L. J. Chen, and Z. L. Wang, *Chem. Phys. Lett.* 435, 119 **(2007)**.

Delivered by Ingenta to: Nanyang Technological University IP : 155.69.4.4 Mon, 10 May 2010 07:45:18

108. R. Ghosh and D. Basak, *Appl. Phys. Lett.* 90, 243106 (**2007**).
109. G. Zhen, Z. Dongxu, L. Yichun, S. Dezhen, Z. Jiying, and L. Binghui, *Appl. Phys. Lett.* 93, 163501 (**2008**).
110. X. Y. Bao, C. Soci, D. Susac, J. Bratvold, D. P. R. Aplin, W. Wei, C. Y. Chen, S. A. Dayeh, K. L. Kavanagh, and D. L. Wang, *Nano Lett.* 8, 3755 (**2008**).
111. T. Martensson, C. P. T. Svensson, B. A. Wacaser, M. W. Larsson, W. Seifert, K. Deppert, A. Gustafsson, L. R. Wallenberg, and L. Samuelson, *Nano Lett.* 4, 1987 (**2004**).
112. E. P. A. M. Bakkers, M. T. Borgström, and M. A. Verheijen, *MRS Bull.* 32, 117 (**2007**).
113. R. G. Driggers, Encyclopedia of Optical Engineering, Marcel Dekker, New York (**2003**).
114. A. G. Milnes and D. L. Feucht, Heterojunctions and Metal-Semiconductor Junctions, Academic Press, New York (**1972**).
115. Y. Gu, E. S. Kwak, J. L. Lensch, J. E. Allen, T. W. Odom, and L. J. Lauhon, *Appl. Phys. Lett.* 87, 043111 (**2005**).
116. Y.-J. Doh, K. N. Maher, L. Ouyang, C. L. Yu, H. Park, and J. Park, *Nano Lett.* 8, 4552 (**2008**).
117. Z. Y. Zhang, C. H. Jin, X. L. Liang, Q. Chen, and L. M. Peng, *Appl. Phys. Lett.* 88, 073102 (**2006**).
118. Z. M. Liao, K. J. Liu, J. M. Zhang, J. Xu, and D. P. Yu, *Phys. Lett. A* 367, 207 (**2007**).
119. Z.-M. Liao, J. Xu, J.-M. Zhang, and D.-P. Yu, *Appl. Phys. Lett.* 93, 023111 (**2008**).
120. G. Cheng, Z. Li, S. Wang, H. Gong, K. Cheng, X. Jiang, S. Zhou, Z. Du, T. Cui, and G. Zou, *Appl. Phys. Lett.* 93, 123103 (**2008**).
121. O. Harnack, C. Pacholski, H. Weller, A. Yasuda, and J. M. Wessels, *Nano Lett.* 3, 1097 (**2003**).
122. K. Cheng, G. Cheng, S. J. Wang, L. S. Li, S. X. Dai, X. T. Zhang, B. S. Zou, and Z. L. Du, *New Journal of Physics* 9, 214 (**2007**).
123. Y. W. Heo, L. C. Tien, D. P. Norton, S. J. Pearton, B. S. Kang, F. Ren, and J. R. LaRoche, *Appl. Phys. Lett.* 85, 3107 (**2004**).
124. K. Keem, H. Kim, G.-T. Kim, J. S. Lee, B. Min, K. Cho, M.-Y. Sung, and S. Kim, *Appl. Phys. Lett.* 84, 4376 (**2004**).
125. Y. W. Heo, L. C. Tien, Y. Kwon, D. P. Norton, S. J. Pearton, B. S. Kang, and F. Ren, *Appl. Phys. Lett.* 85, 2274 (**2004**).
126. A. Francinelli, D. Tonneau, N. Clement, H. Abed, F. Jandard, S. Nitsche, H. Dallaporta, V. Safarov, and J. Gautier, *Appl. Phys. Lett.* 85, 5272 (**2004**).
127. A. Fujiwara, K. Yamazaki, and Y. Takahashi, *Appl. Phys. Lett.* 80, 4567 (**2002**).
128. G. N. Gol'tsman, O. Okunev, G. Chulkova, A. Lipatov, A. Semenov, K. Smirnov, B. Voronov, A. Dzardanov, C. Williams, and R. Sobolewski, *Appl. Phys. Lett.* 79, 705 (**2001**).
129. J. K. W. Yang, E. Dauler, A. Ferri, A. Pearlman, A. Verevkin, G. Gol'tsman, B. Voronov, R. Sobolewski, W. E. Keicher, and K. K. Berggren, *IEEE Transactions on Applied Superconductivity* 15, 626 (**2005**).
130. K. M. Rosfjord, J. K. W. Yang, E. A. Dauler, A. J. Kerman, V. Anant, B. M. Voronov, G. N. Gol'tsman, and K. K. Berggren, *Opt. Express* 14, 527 (**2006**).
131. F. Marsili, D. Bitauld, A. Fiore, A. Gaggero, F. Mattioli, R. Leoni, M. Benkahoul, and F. Levy, *Opt. Express* 16, 3191 (**2008**).
132. S. Miki, M. Fujiwara, M. Sasaki, B. Baek, A. J. Miller, R. H. Hadfield, S. W. Nam, and Z. Wang, *Appl. Phys. Lett.* 92, 061116 (**2008**).
133. E. A. Dauler, A. J. Kerman, B. S. Robinson, J. K. W. Yang, B. Voronov, G. Goltsman, S. A. Hamilton, and K. K. Berggren, *Journal of Modern Optics* 56, 364 (**2009**).
134. I. Milostnaya, A. Korneev, M. Tarkhov, A. Divochiy, O. Minaeva, V. Seleznev, N. Kaurova, B. Voronov, O. Okunev, G. Chulkova, K. Smirnov, and G. Gol'tsman, *J. Low Temp. Phys.* 151, 591 (**2008**).
135. C. Zinoni, B. Alloing, L. H. Li, F. Marsili, A. Fiore, L. Lunghi, A. Gerardino, Y. B. Vakhtomin, K. V. Smirnov, and G. N. Gol'tsman, *Appl. Phys. Lett.* 91, 031106 (**2007**).
136. N. Garcia, J. Przeslawski, and M. Sharonov, *Surf. Sci.* 407, L665 (**1998**).
137. J. L. Sun, X. Zhao, and J. L. Zhu, *Nanotechnology* 19, 085703 (**2008**).
138. M. S. Hu, H. L. Chen, C. H. Shen, L. S. Hong, B. R. Huang, K. H. Chen, and L. C. Chen, *Nat. Mater.* 5, 102 (**2006**).
139. D. A. B. Miller, *Proceedings of the IEEE* 88, 728 (**2000**).
140. J. B. Baxter and C. A. Schmuttenmaer, *J. Phys. Chem. B* 110, 25229 (**2006**).
141. K. Nikolić and M. Forshaw, *From nanostructures to nanosensing applications : proceedings of the International School of Physics "Enrico Fermi", Varenna on Lake Como, Villa Monastero, July 2004*, edited by A. D'Amico, A. Paoletti, G. Balestrino, and Società italiana di fisica, IOS Press, Societa Italiana di Fisica, Amsterdam, Netherlands, Washington, DC, Bologna, Italy (**2005**).
142. H. J. Fan, P. Werner, and M. Zacharias, *Small* 2, 700 (**2006**).
143. D. Whang, S. Jin, Y. Wu, and C. M. Lieber, *Nano Lett.* 3, 1255 (**2003**).
144. D. Whang, S. Jin, and C. M. Lieber, *Jpn. J. Appl. Phys., Part 1* 43, 4465 (**2004**).
145. C. S. Lao, J. Liu, P. Gao, L. Zhang, D. Davidovic, R. Tummala, and Z. L. Wang, *Nano Lett.* 6, 263 (**2006**).
146. G. Yu, A. Cao, and C. M. Lieber, *Nat. Nano* 2, 372 (**2007**).
147. Z. Fan, J. C. Ho, Z. A. Jacobson, R. Yerushalmi, R. L. Alley, H. Razavi, and A. Javey, *Nano Lett.* 8, 20 (**2008**).
148. Y. Roie, A. J. Zachery, C. H. Johnny, F. Zhiyong, and J. Ali, *Appl. Phys. Lett.* 91, 203104 (**2007**).
149. Z. Fan, J. C. Ho, Z. A. Jacobson, H. Razavi, and A. Javey, *Proceedings of the National Academy of Sciences* (**2008**), Vol. 105, p. 11066.
150. J. H. Park, S. H. Seo, I. S. Wang, H. J. Yoon, J. K. Shin, P. Choi, Y. C. Jo, and H. Kim, *Jpn. J. Appl. Phys., Part 1* 43, 2050 (**2004**).
151. T. Martensson, P. Carlberg, M. Borgstrom, L. Montelius, W. Seifert, and L. Samuelson, *Nano Lett.* 4, 699 (**2004**).
152. A. I. Hochbaum, R. Fan, R. R. He, and P. D. Yang, *Nano Lett.* 5, 457 (**2005**).

Delivered by Ingenta to: Nanyang Technological University IP : 155.69.4.4 Mon, 10 May 2010 07:45:18

Received: 3 February 2009. Accepted: 31 March 2009.